

DESIGN AND CONSTRUCTION OF A  
LOW EARTH ORBIT SATELLITE  
GROUND STATION

by  
Eric Darnel

RECOMMENDED:

John Aspnes  
[Signature]

Joseph S. Hawkins  
Advisory Committee Chair

John Aspnes  
Department Head

APPROVED:

[Signature]  
Dean, College of Science, Engineering and Mathematics

[Signature]  
Dean of the Graduate School

12-5-00  
Date

DESIGN AND CONSTRUCTION OF A LOW EARTH ORBIT SATELLITE  
GROUND STATION

A  
THESIS

Presented to the Faculty  
of the University of Alaska Fairbanks  
in Partial Fulfillment of the Requirements  
for the Degree of

MASTER OF SCIENCE

By  
Eric Darnel, B.S.E.E

Fairbanks, Alaska

December 2000

ALASKA  
TL  
796.5  
U6  
C58  
2000



## **Abstract**

This thesis describes the design and construction of a satellite ground station constructed in support of the Citizen Explorer Program. The University of Alaska Fairbanks was chosen to participate in this program due to its latitude that gives it excellent access to polar-orbiting satellites.

The advantage that higher latitudes have in accessing low earth orbiting satellites is examined. It is demonstrated that Fairbanks, Alaska has roughly twice the access to polar orbiting satellites than the mid-latitudes of the contiguous US.

Link budgets for the communication system were developed, which led to the construction of helical antennas to communicate with the satellite. Data are presented that demonstrate the antennas, as well as the rest of the satellite tracking system, functioned acceptably.

The satellite ground station will provide internet access to the spacecraft. The procedure used to test this approach and its results are given, as well as recommendations for future work.

# Contents

<b>1</b>	<b>Introduction</b>	<b>1</b>
1.1	Citizen Explorer Project . . . . .	1
1.2	Satellite Overview . . . . .	2
1.3	Ground Station Overview . . . . .	3
<b>2</b>	<b>Spacecraft Orbit</b>	<b>7</b>
<b>3</b>	<b>Spacecraft Communication Link</b>	<b>10</b>
3.1	Communications Overview . . . . .	10
3.2	Probability of Bit Error . . . . .	14
3.3	Remarks . . . . .	32
<b>4</b>	<b>Antennas</b>	<b>33</b>
4.1	Antenna Design . . . . .	33
4.2	Antenna Steering . . . . .	37
4.3	Antenna Testing . . . . .	39
<b>5</b>	<b>Ground Station Testing</b>	<b>42</b>
5.1	Testing the Tracking System . . . . .	42
5.2	Testing the Network Interface . . . . .	44
<b>6</b>	<b>Equipment Description</b>	<b>48</b>
<b>7</b>	<b>Conclusions</b>	<b>53</b>
<b>A</b>	<b>Measuring Effects of Intersymbol Interference and Non-linear Channel Effects</b>	<b>54</b>
<b>B</b>	<b>Measuring Receiver Noise Temperature</b>	<b>58</b>
<b>C</b>	<b>Downlink Budget Calculations</b>	<b>61</b>
	<b>References</b>	<b>64</b>

## List of Figures

1	Overview of Citizen Explorer project . . . . .	2
2	Basic block diagram of ground station . . . . .	4
3	Screen shot of SatTrack interface . . . . .	6
4	Illustration of inclination angle . . . . .	7
5	Satellite availability versus latitude of ground station . . . . .	8
6	Average time to wait for a 5-minute pass for the CX-1 orbit . . . . .	9
7	Top level view of overall communications between spacecraft and control facilities . .	11
8	Spacecraft communication block diagram . . . . .	11
9	Error performance of MSK and GMSK, both coherently and non-coherently detected	17
10	Illustration of slant range and angle of elevation for the CX-1 orbit . . . . .	19
11	Illustration of slant range variables . . . . .	20
12	Path loss for the CX-1 signal links . . . . .	20
13	Illustration of receive system . . . . .	22
14	Spacecraft transmit antenna gain as a function of elevation angle . . . . .	25
15	Baseband transceiver channel response. . . . .	31
16	Photograph of antennas . . . . .	34
17	Diagram of helical antenna . . . . .	35
18	Top view of 435 MHz antenna base . . . . .	36
19	Bottom view 435 MHz antenna base . . . . .	37
20	Azimuth plot of 145 MHz helical antenna data . . . . .	39
21	Azimuth plot of 435 MHz helical antenna data . . . . .	40
22	Return loss measurements of 145 MHz antenna . . . . .	41
23	Return loss measurements of 445 MHz antenna . . . . .	41
24	Testing the network interface in tiers . . . . .	44
25	Graphical interface for serial line switcher . . . . .	46
26	Baseband frequency response of transceivers . . . . .	47
27	Photograph of ground station equipment . . . . .	48
A.1	Setup for measuring bit error rate . . . . .	54
A.2	AX.25 'Unnumbered Information' packet structure. . . . .	55

A.3	Simulation results validating the derived relationship between packet success rate and probability of bit error. . . . .	56
B.4	Set up for measuring receiver noise temperature . . . . .	58
B.5	Ideal and empirical data for determining receiver noise figure . . . . .	59

## List of Tables

I	Downlink budget . . . . .	24
II	Uplink budget . . . . .	29
III	Antenna parameters . . . . .	36
IV	ICOM 821H transceiver specifications . . . . .	49
V	Attenuation for different 50 $\Omega$ cable types . . . . .	52
VI	RG-8/U cables produced by Belden . . . . .	52

# 1 Introduction

## 1.1 Citizen Explorer Project

The University of Colorado Boulder plans to launch a spacecraft known as Citizen Explorer 1 (CX-1). The Citizen Explorer project was created to foster collaboration between colleges, grade schools, and the space industry. The project is funded by the Colorado Space Grant Consortium and the spacecraft is being constructed by students at the University of Colorado, Boulder. The CX-1 payload will measure solar ultraviolet radiation and atmospheric ozone with two onboard photospectrometers and relay this information to grade schools around the world. Each participating grade school will have an inexpensive receiving station from which students will monitor atmospheric ozone and ultraviolet data over their schools. The grade schools will additionally have handheld instruments that perform ultraviolet and aerosol measurements. Data from the spacecraft as well as the handheld instrument data will be relayed to the University of Colorado via the internet. In essence, a global atmospheric sensor system will be employed. A block diagram of the satellite-ground station portion of the project is shown in Figure 1. The satellite payload portion of the project is designed and built by student using donations and assistance from the commercial spacecraft industry, which will then benefit from well experienced college graduates.

The Alaska Space Grant Program came to participate in the Citizen Explorer project by the nature of the spacecraft's orbit. The CX-1 orbit will be in a near-polar, low-earth, sun-synchronous (10 am and 10 pm) orbit, giving northerly and southerly latitudes more exposure to the spacecraft. The satellite's orbit is further described in Section 2. A ground control station was built atop the engineering building at the University of Colorado at Boulder (40° N). A second ground control station was desired at a high latitude to provide redundancy and extend coverage when the satellite could not be seen from lower latitudes. The University of Alaska Fairbanks was an excellent choice for the location of the second ground station due to the northern latitude of Fairbanks, Alaska (65° N) and the nature of the satellite's orbit. The Citizen Explorer Alaska ground station was funded by the Alaska Space Grant Program and the design and implementation of this ground station is the topic of this thesis.



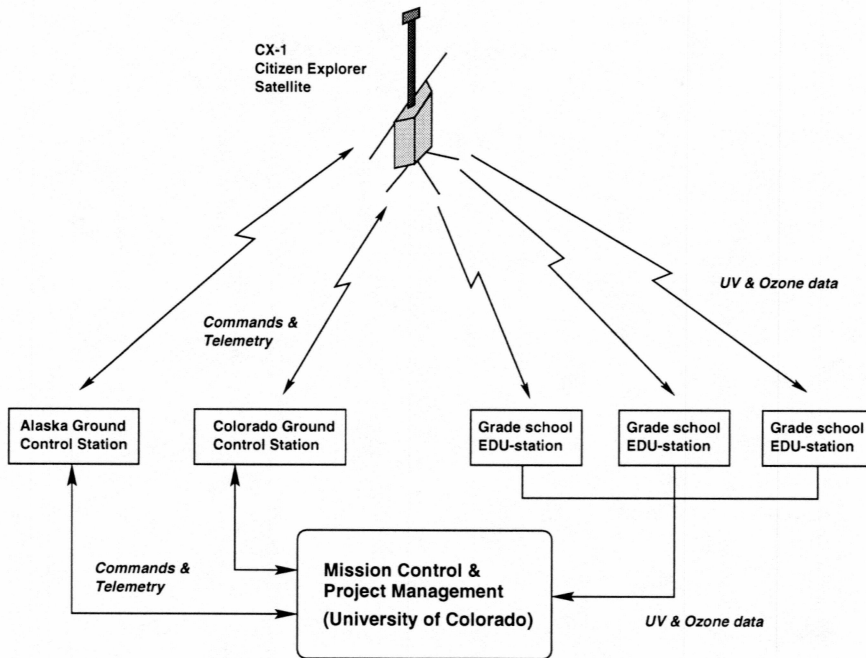


Figure 1: Overview of Citizen Explorer project

## 1.2 Satellite Overview

To quantify the requirements of the ground station, a description of the satellite and its orbit is warranted. The mass of the CX-1 spacecraft is about 40 kg and will be placed in a Low Earth Orbit at about 706 km above the Earth, yielding an orbital period of about 98 minutes, or about 14.6 orbits per day. The longest pass that a ground observer can see the satellite will be about 15 minutes. Two photospectrometers will be carried on board; one will measure the 280 - 350 nm region and the other is a narrowband spectrometer at 365 nm.

The satellite will transmit on 436.75 MHz, in the 70-cm amateur radio band, and receive on 145.86 MHz, in the 2-meter amateur radio band. The modulation format will be Gaussian Minimum Shift Keying (GMSK) at 9600 baud. The transmission bandwidth was set to match the passband of available amateur radio equipment, which is about 15 kHz.

The satellite will receive with a quarter-wave dipole and transmit with an omnidirectional turnstile-type antenna configured for left handed circular polarization (LHCP). The transmit power will be nominally 2 Watts.

The flight computer will use the VxWorks operating system, a real-time operating system used

in many scientific applications. The software for communicating with the spacecraft is being written to use TCP/IP (Transmission Control Protocol/Internet Protocol). Therefore a network interface to the satellite must be established for the communication software to operate.

## **1.3 Ground Station Overview**

### **1.3.1 Ground Station Requirements**

The ground station software was written by student and staff at the University of Colorado for the Linux operating system, as Linux has proven to be a reliable and versatile operating system. Preliminary radio link calculations showed that low-gain fixed antennas at the ground station would not suffice and that directive, steerable antennas would be required. Considering this, the requirements for the ground control station may be summarized as follows:

1. Provide a sufficiently strong signal link to and from the satellite
2. Provide a means for pointing the antennas at the satellite (tracking).
3. Provide a means of establishing a network interface to the satellite.

Figure 2 illustrates how the ground station will serve to satisfy these requirements. These requirements are discussed with more detail in the following subsections.

### **1.3.2 Communication Link**

#### **Communication Software**

The command and telemetry software, which is currently being written at the University of Colorado, will interface to the spacecraft via an internet address provided by the ground station. The communication software will be run on a machine at the University of Colorado, completely independent of the ground station operations. Thus, no further mention is made of the communication software used to control the satellite.

#### **Signal Link**

Signal strength calculations showed that both the uplink and downlink would be best served by antennas with appreciable gain, which must be actively pointed at the satellite. Since broad or multi-

band antennas at these frequencies and required gains are not known to exist, separate antennas were required for uplink and downlink.

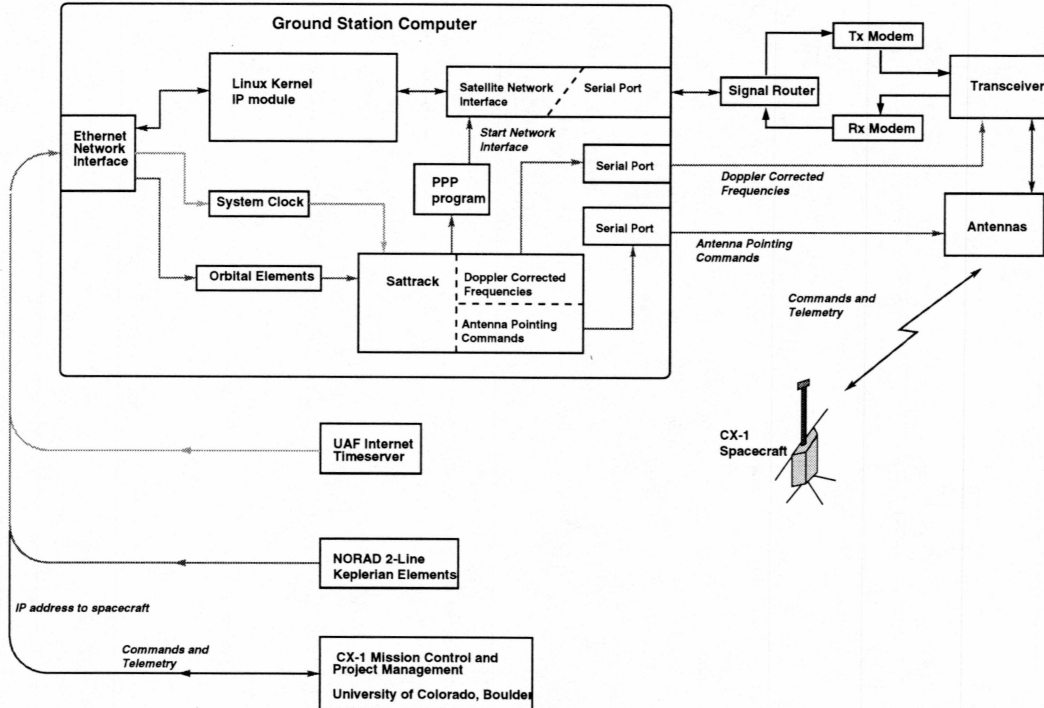


Figure 2: Basic block diagram of ground station

A link budget was generated for this project, and is presented in Section 3. After considering the link budget requirements, both antennas were chosen to be circularly polarized monofilar helical antennas. The uplink budget showed that sufficient ground station transmit power was readily available from amateur radio transceivers. The antennas were mounted on a mast/boom combination with motors to control azimuth and elevation for antenna pointing.

Another consideration was Doppler frequency shift. A satellite in Low Earth Orbit has considerable velocity, and causes frequency shift in signals that is proportional to the relative speed of the satellite and frequency used. The Doppler shift on the uplink frequency of 145.86 MHz is about 3 kHz, which is nearly small enough to ignore considering the bandwidth of the signals. However the Doppler shift of the downlink frequency is about 10 kHz, and frequency must be corrected throughout the satellite passes. Doppler-shift corrected uplink and downlink frequencies will be maintained by satellite tracking software running on the ground station computer, as described in the next section.

### 1.3.3 Satellite Tracking

Tracking a Low Earth Orbiting satellite requires the following considerations:

1. Maintaining accurate satellite orbital data
2. Maintaining accurate time
3. Antenna pointing
4. Doppler shift correction

In order to predict the position of a satellite, a set of orbital parameters, usually in the form of Keplerian elements, must be available. These describe the satellite's orbit, and could be used indefinitely if there were no uncertainty in the figures and there were no perturbations from the model that Keplerian elements are based upon. In practice, a set of Keplerian elements may reliably predict a satellite's position for more than a week, depending upon the accuracy required. Orbital elements are typically available in the form of "Two line elements," an ASCII text segment of only two lines. The two line elements for CX-1 will be generated by NORAD, and downloaded daily via internet into the ground control station.

Accurate time keeping is essential to satellite orbital prediction. Accurate time is maintained within the ground control station computer using an internet time server. The UAF time server, "ntp.alaska.edu," is maintained by GPS clock signals. The ground station computer runs a program that maintains synchronization of the operating system clock with the time server.

Antenna pointing utilizes software and a steerable antenna system. The tracking software, SatTrack <sup>1</sup>Version 3, is a free and open source satellite tracking program. SatTrack takes two line elements from a file and predicts azimuth and elevation angles of satellites in real time. The program was adapted to send the azimuth and elevation data to one of the computer's serial communication ports for antenna steering. The SatTrack code was further modified to send corrected uplink and downlink frequency information to another serial communication port, to which the ground station transceiver was connected<sup>2</sup>. Figure 3 shows a screen shot of the SatTrack's user interface.

A 'TrakBox' kit was assembled to serve as an interface between the computer and antenna pointing motors. This received the azimuth and elevation commands from SatTrack.

<sup>1</sup>Developed by Manfred Bester, Bester Tracking Systems, Inc.

<sup>2</sup>Fernando Mederos, CX6DD, modified SatTrack to control an Icom 821H transceiver

```

SatTrack V3.1          F0-20 TRACKING DISPLAY          STATION_ID
-----
Ground Stn : Fairbanks Now: Thu 06Apr2000 Downlnk USB : 435.8500 MHz
Satellite  : JAS-B 97 10:05:30 AST Uplink LSB : 145.9500 MHz
Inclination: 99.042 deg Downlnk Loss: 0.0000 dB
Orbit      : 47613 21.2 % D Object : 20480 Uplink Loss: 0.0000 dB
Sun Az/El: 132.8 25.0 deg Model : SGP4 Sun Angle : 65.9170 deg
Moon Az/El: 104.2 18.2 deg Tracking: OFF Phase ( 256): 54.2800 J

Azimuth   : 226.134 deg Latitude   : 59.618 deg S /
Elevation : -66.298 deg / Longitude  : 135.519 deg E
Range     : 13020.199 km Height      : 1269.321 km
Range Rate: -0.956 km/s Velocity   : 7.254 km/s

State Vector X: -855.077 km Y: -3783.113 km Z: -6578.595 km
              VX: -3.538 km/s VY: -5.484 km/s VZ: +3.167 km/s

Next AOS : 97/10:52:39 AST AOS Azimuth : 347.600 deg D
Duration : 0/00:10:19 MEL Azimuth : 14.700 deg D
Next LOS : 97/11:02:59 AST LOS Azimuth : 42.900 deg D
Countdown: 0/00:47:09 Max Elevation: 3.200 deg
              MEL Range : 4352.700 km

_Ground Track: PD70S3 1493.7 km MSM of Macquarie Island (Australia)

```

Figure 3: Screen shot of SatTrack interface

### 1.3.4 Network Interface to Spacecraft

Ultimately, the ground station's end function will be to provide internet access to the spacecraft via a standard Internet Protocol (IP) address. An internet network interface to the spacecraft was established using common Point-to-Point Protocol (PPP) programs in the Linux ground station and in the VxWorks flight software. By default, establishment of a PPP link allows the ground station to communicate with the spacecraft, but no other hosts. To extend access to the general internet, proxy Address Resolution Protocol (ARP) was used. In effect, the ground station will act as a gateway that will forward IP traffic to the spacecraft. Naturally, the forwarding will be limited to the host that is running the communication software. The net effect of these efforts is to make the ground station transparent to the command and telemetry software running on a remote machine.

PPP requires a digitally transparent serial link between two points to establish a connection. The digitally transparent link is implemented at the ground station using a commercial packet controller/modem that used the AX.25 protocol and GMSK modulation. The spacecraft will have an equivalently configured packet controller/modem, known as the critical decoder. The SatTrack code was modified to run the PPP program whenever the satellite was in view. The PPP program will then transmit data packets to attempt to negotiate a link with the spacecraft. When the spacecraft replies, the two PPP programs will negotiate a network interface that is used by the TCP/IP communication software.



## 2 Spacecraft Orbit

The main reason that a ground station was constructed in Alaska is due to the fact that high latitudes have better access to polar orbiting satellites. This section serves to describe the CX-1 orbit and to quantify this justification for locating a ground station in Fairbanks, Alaska.

A satellite in low earth orbit very nearly describes an ellipse in space, which is slowly perturbed by non-uniform effects of the Earth's gravitational field [Chobotov '91]. The rate at which the satellite must travel to maintain its orbit is inversely proportional to the orbit height. A Low Earth Orbit (LEO) implies that the spacecraft is moving relatively quickly in relation to the Earth surface. If the orbit is nearly circular, as the CX-1 orbit will be, the rate is related to the orbital height by

$$v \cong \sqrt{\frac{\mu}{R_e + h}} \quad (1)$$

where  $v$  is the spacecraft's speed,  $\mu$  is Kepler's constant ( $4 \times 10^5 \text{ km}^3/\text{sec}^2$ ),  $R_e$  is the Earth's radius ( $\cong 6378 \text{ km}$ ), and  $h$  is the orbital height above the Earth. The mean orbital height of the CX-1 orbit will be about 706 km, which gives rise to a speed of about 7.5 km/sec relative to the Earth's surface<sup>3</sup>.

If the plane of a LEO orbit does not lie in the equatorial plane, the ground track of the satellite will trace a pattern in the likeness of Figure 4 (a), which shows that sooner or later, the satellite will pass over a large portion of the Earth. If global access to the satellite is desired, a large inclination angle ( $\Theta_i$ ) is used as shown in Figure 4 (b).



Figure 4: Illustration of inclination angle

The plane of the orbit will be inclined at an angle of  $98.3^\circ$  from the equatorial plane. The fact

<sup>3</sup>This does not take into account rotation of Earth



that the angle of inclination was greater than  $90^\circ$  implies that the spacecraft's track moved opposite to the Earth's rotation; this is known as a retrograde orbit. The combination of the orbital height and the particular inclination angle of  $98.3^\circ$  gives rise to a sun-synchronous orbit: the ground track of the satellite repeats itself each day. This is made possible by the precession of the orbital plane due to oblateness of the Earth. The amount of precession is a function of inclination and orbital height [Chobotov '91]. An inclination angle of  $98.3^\circ$  and an orbital height of 706 km yields precession of 1 revolution in one year, or about  $1^\circ$  per day. The effect of this is that the satellite's pass over a ground station occurs at the same local time each day, which makes communication more convenient. This feature of the orbit lends itself well to grade school activities that are best scheduled at regular daily times. Specifically, the CX-1 orbit is planned to be placed in a 10 am - 10 pm sun synchronous orbit.

In order to quantify the advantage of latitude for a ground station, Matlab software was used to simulate the CX-1 orbit. The angle of elevation (angular distance from Earth surface tangent) was recorded for varying ground station latitudes. The results of this simulation are shown in Figure 5.

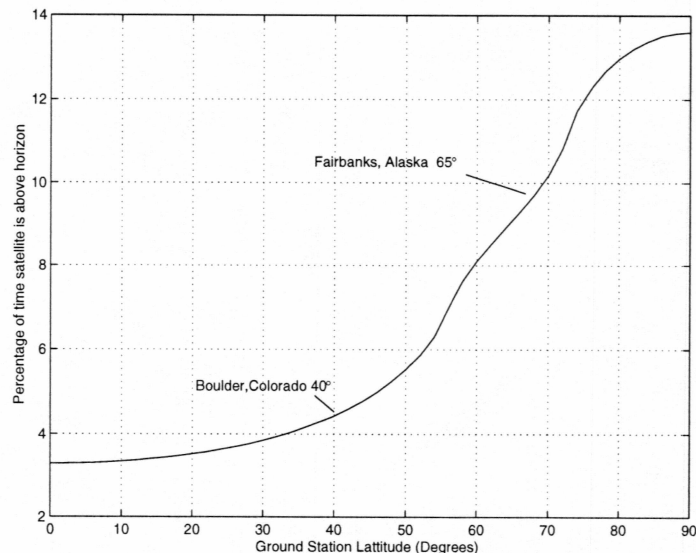


Figure 5: Satellite availability versus latitude of ground station

The availability is statistically defined here to be the fraction of time that the satellite is above the horizon of a ground station. The simulation performed here assumed that the horizon of the ground station was not obstructed. For a satellite in an orbit 700 km above the Earth, the maximum availability was found to be about 14%, if the station was placed at a pole. The availability of

the CX-1 ground station in Fairbanks, Alaska is shown to be 8.6% while the availability from the University of Colorado (Boulder, Colorado) was 4.3%.

It is also informative to analyze availability information in a different manner. The average wait time for a reasonable pass could also be considered a figure of merit for a ground station, if for instance a need arose to quickly communicate with the spacecraft. To illustrate this, the same Matlab routine was applied in a different manner to observe the average time that a ground station would have to wait for a reasonable pass, which was considered to be a pass for which the satellite is above the horizon for more than 5 minutes. Figure 6 shows a curve fit for these simulation results<sup>4</sup>.

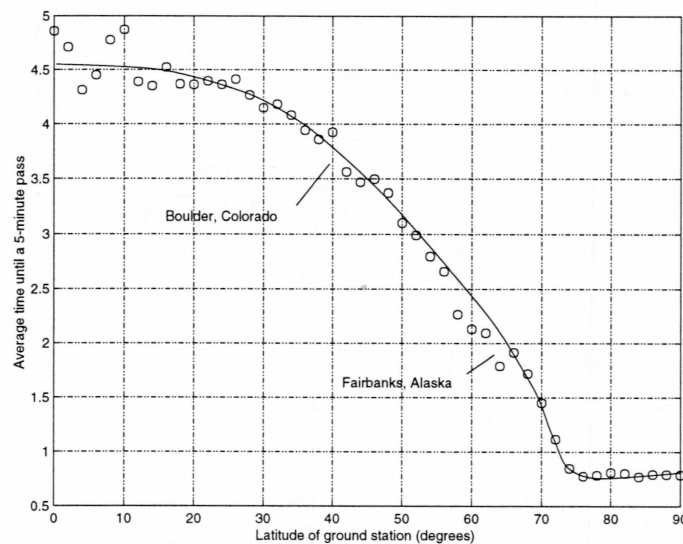


Figure 6: Average time to wait for a 5-minute pass for the CX-1 orbit

Note that Boulder, Colorado had a mean wait time of about 3.7 hours, while Fairbanks, Alaska had a mean wait time of about 2.0 hours. This can be converted to an expected number of acceptable passes per day for each ground station by dividing 24 hours by the mean wait time. The result is that the Colorado ground station can expect about 6 passes per day that are at least 5 minutes in duration and the Alaska ground station can expect about 12 passes per day.

Thus, the ground station at the University of Alaska Fairbanks not only provided redundancy for the CX-1 spacecraft, but will be doubly capable of communicating with it<sup>5</sup>.

<sup>4</sup>Figure 6 shows the mean of many simulations, of which there was a large statistical variance.

<sup>5</sup>The assumption was made that each ground station had an unobstructed view of the horizon.

### 3 Spacecraft Communication Link

A critical factor in communications system design is an appropriate link budget that describes the quality of information transfer. For the Citizen Explorer ground control stations, there are two link budgets, one for uplink and one for downlink. A well designed satellite communication system is downlink limited, meaning that the link quality is limited by the spacecraft and not the ground station. When the costs of ground station equipment are compared to costs of flight hardware, the reason for a downlink limited system becomes apparent.

The ultimate figure of merit for a link budget is called the margin of signal strength above the minimum required for satisfactory communications. For a digital communication system, the final figure of merit is the probability of bit error, which is commonly labeled as the bit error rate (BER). This section describes the communications link between the spacecraft and the ground station and derives the link budget for the VHF/UHF frequencies used with CX-1.

#### 3.1 Communications Overview

All in all, the ground station will act as a simplified IP router for the spacecraft. A top level view of the whole communication system is depicted in Figure 7. The interface between the control facility computer and the ground station is via standard internetworking and warrants no further discussion except that the control facility will expect the IP address of the spacecraft to be valid when the spacecraft is in view of the ground station. The IP address assigned by this ground station is expected to be 137.229.61.65 and associated with hostname cx1.ee.uaf.edu. For security reasons, the ground station's IP module will only forward traffic to the spacecraft that originates from the control facility's IP address at the University of Colorado, Boulder.

Communications with the spacecraft may be viewed in terms of the 5-layer TCP communication model. The 5-layer TCP/IP communication model has become the working standard, in comparison to its academic predecessor, the OSI 7-layer communication model [Stallings '97]. The TCP/IP protocol model elements can be related to the ground station construction as shown in Figure 8.

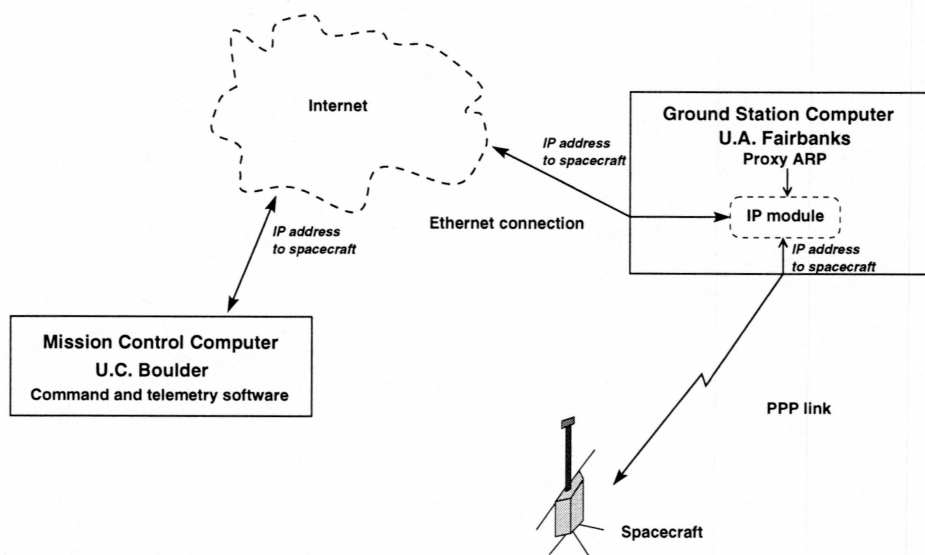


Figure 7: Top level view of overall communications between spacecraft and control facilities

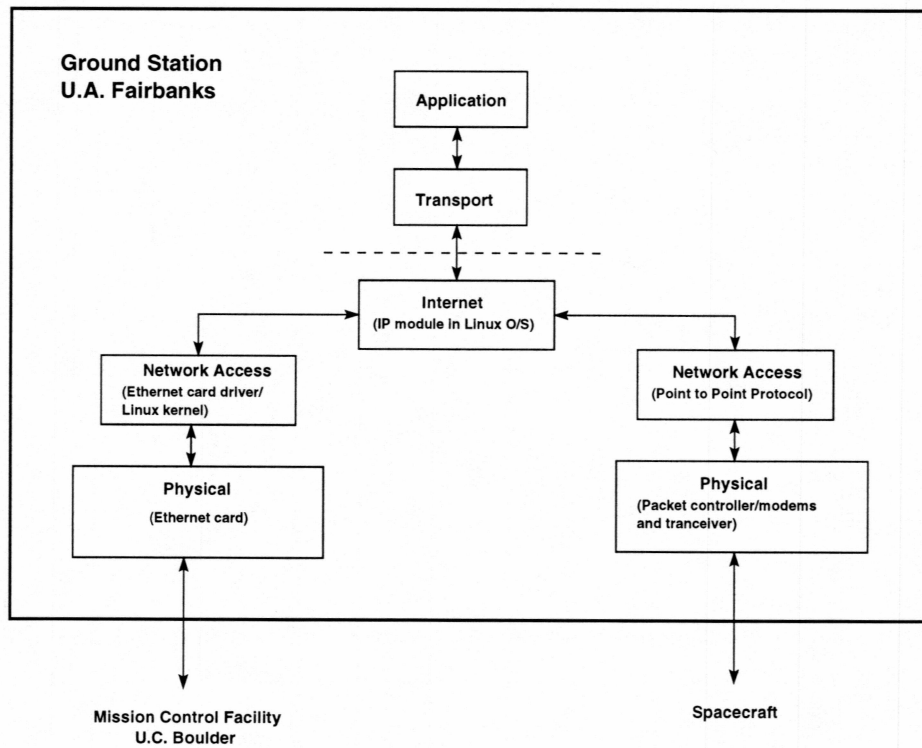


Figure 8: Spacecraft communication block diagram

### **Application Layer**

The application layer involves the use of end level applications, which corresponds to the command and telemetry software run at the mission control facility. This is completely decoupled from the ground station, except that the ground station will relay traffic between this software and the satellite.

### **Transport Layer**

The transport layer involves protocols such as Transmission Control Protocol (TCP) and User Datagram Protocol (UDP). TCP is a protocol that guarantees delivery of messages and involves acknowledgement and retransmission. In contrast, UDP does not guarantee delivery .

Note that the Application and Transport layers of Figure 8 are divided from the rest of the communication system. This is done to show that these layers will not be used in the ground station, since the TCP-based command and telemetry software will be run remotely at the University of Colorado.

Central to the ground station is the Internet Protocol (IP) module of the computer operating system. The IP module is responsible for routing data based upon IP addresses and routes data to the appropriate Network Access device. The IP module recognizes data bound for the spacecraft from the ethernet devices and routes them to the Point to Point Protocol (PPP) device and vice versa. Internet Protocol does not provide any guarantee of message delivery. This is left to the Transport or Application layers.

### **Network Access Layer**

Two Network Access devices are present in the ground station, one for the ethernet interface and one for the PPP interface. The ethernet card driver serves as the interface between the IP module and the network interface card. The PPP program fills a similar role for a serial port. The PPP link establishment can be further decomposed into three distinct processes [RFC 1661].

1. Encapsulation
2. Link control protocol
3. Network control protocol



**Encapsulation** PPP encapsulation is a variant of High-Level Data Link Control (HDLC), which is a common protocol upon which many network access protocols are based [Stallings '97]. Encapsulation refers to the method by which data is placed into frames to include start and stop flags, address, control, data, and Frame Check Sequence (FCS) information [RFC 1662]. PPP fixes the address and control bytes, so that their HDLC-intended functions are not variable. The address is fixed at hex value FF and the control byte corresponds to an *Unnumbered* HDLC frame, which requires no acknowledgement frames in return. Therefore, addressing (to include routing) and delivery acknowledgement are left to higher level protocols, namely IP and TCP respectively, in this use of PPP.

**Link Control Protocol** In PPP link establishment, the link control protocol (LCP) is first used to verify the presence and identity of a PPP peer and establish parameters for the link such as compression, maximum transmit unit length (MTU), and the method of authentication. LCP is also used to terminate the PPP link.

**Network Control Protocol** After LCP is satisfied, Network Control Protocol is then used to negotiate an IP channel between the remote and local host. The IP addresses for the ground station and spacecraft are stored in a PPP configuration file on the ground station. IP is only one Network Layer Protocol that may be carried via PPP. Once completed, the computer operating system kernel is aware of the IP addresses assigned at either end of the PPP interface. The IP address used for the ground station in the PPP link is the same that is used on the ground station's ethernet interface.

### Physical Layer

The Physical Interfaces are an IEEE 802.3 ethernet interface and the interface presented by the combination of packet controller/modem and transceiver. The packet controller/modems provided an addition level of encapsulation. The packet controller/modems were used to transparently generate and decode AX.25 Unnumbered Information (UI) Frames.

Like PPP, AX.25 (*Amateur X.25*) is also based upon HDLC [Beech '97]. The primary feature is that 14 to 28 bytes are allowed in the address field, which are used for amateur radio user call signs. Again, since acknowledgment was performed at higher levels, unnumbered frames were used, though there are two other types of AX.25 frames available.



Not yet described is Address Resolution Protocol (ARP). This is the mechanism by which ethernet (also called hardware or MAC) addresses are associated with IP addresses. In order for traffic from the control facility host to reach the spacecraft, the ethernet address of the ground station must be associated with the spacecraft's IP address, since the PPP link has no ethernet address of its own. This is done simply by invoking the PPP program with the instruction to add the PPP link to the ground station ARP table.

For the entire system to work, the data must be conveyed with an acceptably low rate of bit errors, as discussed in the following section.

### 3.2 Probability of Bit Error

A measure of the quality of a digital communication system may be stated as the rate at which errors occur in the recovered data, or equivalently, the probability of a single bit being in error. This probability of bit error  $P_e$  is commonly labeled as the Bit Error Rate (BER). The rate at which errors in the channel occur can be forecast with statistical knowledge of the system. Major contributors to the errors include:

1. Noise
2. Intersymbol interference
3. External interference
4. Nonlinear channel effects

Each of these issues are addressed in the following sections. Each source of errors listed above is independent of one another, and therefore the probability of a recovered bit being in error is the sum of each of the individual probabilities [Ho '70]. Any effect by itself may limit the quality of the link. This is illustrated by expressing the probability of a single bit being in error as the sum of all possible independent error sources:

$$P_e = \sum_{i=1}^N P_i \quad (2)$$

where  $P_i$  is the  $i^{th}$  source of error probability and  $P_e$  is the net bit error probability. For instance, consider the contributions from noise and intersymbol interference. The probability of bit error

from intersymbol interference is often fixed by the bandwidth and frequency response of the system equipment. The probability of bit error from noise is variable, because increasing signal strength will decrease this probability. Therefore, one may take measures to increase the link quality by increasing the received signal strength, but these efforts will be fruitless if the system is limited by intersymbol interference.

### 3.2.1 Probability of Bit Error due to Noise and Link Budget

The final figure of merit in a noise limited link budget is the ratio of energy per bit received to the spectral density of received noise power, or  $\frac{E_b}{N_o}$ . This represents the signal quality at a point in the system just prior to demodulation. If the noise is white Gaussian noise, the expected Bit Error Rate can be derived in terms of  $\frac{E_b}{N_o}$ . This relationship is determined by the modulation format used. In all cases, the probability of bit error ( $P_e$ ) is an inverse relationship to  $\frac{E_b}{N_o}$ .

The object of a link budget is to determine the value of  $\frac{E_b}{N_o}$  expected under normal operating conditions and compare it to the required value of  $\frac{E_b}{N_o}$  to attain a given bit error probability. The difference between the received  $\frac{E_b}{N_o}$  and the required  $\frac{E_b}{N_o}$  for a certain  $P_e$  is labeled as the bit error rate margin.

From an engineering perspective, it is not necessary or economically efficient to produce the lowest value of  $P_e$  possible. Using a protocol that can deal with a reasonable  $P_e$  produces the best compromise between performance and equipment costs.

The relationship between  $P_e$  to  $\frac{E_b}{N_o}$  depends upon the modulation format. For CX-1, the modulation format was Gaussian-filtered Minimum Shift Keying (GMSK). The following paragraph develops a sense of GMSK from basic modulation concepts.

A simple method of modulating a carrier with a digital data stream would be to use the binary states of the data to alternate between two different carrier frequencies [Sklar '88]. This is known as *Frequency Shift Keying* (FSK). The two different frequencies may be spaced arbitrarily apart; however, bandwidth and Intersymbol Interference (ISI) must be considered. The wider the frequencies are spaced, the greater the bandwidth of the signal. The 'tone spacing' cannot be arbitrarily reduced without introducing intersymbol interference. For non-coherently detected FSK signals (as in amateur radio equipment), the minimum tone spacing is  $\frac{1}{T}$  where  $T$  is the bit-time. If the signal can be received coherently (carrier phase is recovered), the tone spacing may be reduced to  $\frac{1}{2T}$  without

introducing intersymbol interference. This gives rise to *Minimum Shift Keying* (MSK). Although MSK is optimally received coherently, it is still recoverable with non-coherent receivers, with some performance loss typically corresponding to about 1 dB of signal strength. The bandwidth may be further reduced by applying the digital data pulses to a low pass filter with a Gaussian response<sup>6</sup> before applying it to a frequency modulator. This form of pulse shaping yields Gaussian filtered Minimum Shift Keying (GMSK) and is suitable for bandwidth-limited environments.

GMSK can be viewed as a degradation from MSK performance [Murota '81]. The relationship between  $P_e$  and  $\frac{E_b}{N_o}$  for non-coherently detected FSK<sup>7</sup> is [Sklar '88]<sup>8,9</sup>

$$P_e = \frac{1}{2}e^{-\frac{1}{2}\frac{E_b}{N_o}} \quad (3)$$

Thus, for GMSK, the relationship may be expressed as

$$P_e = \frac{1}{2}e^{-\frac{1}{2}\frac{E_b}{N_o}d_{MSK}} \quad (4)$$

where  $d_{MSK}$  is the degradation from the MSK performance. The degradation is typically less than 2 dB and the value for  $d_{MSK}$  that corresponds to 2 dB degradation is 0.63. The degradation is justifiable in that the bandwidth of a GMSK signal is much less than that of an MSK signal. The amount of degradation is a function of the rolloff-rate of the Gaussian filter. A flat response, or no filtering, results in no degradation, while steeper filter rolloff increases degradation, but significantly decreases the bandwidth. One way of defining the Gaussian filter response is by its -3 dB bandwidth. This can be normalized by multiplying by the bit time so that the Gaussian filter parameter is  $BT$  where  $B$  is the -3 dB bandwidth of the Gaussian low-pass filter and  $T$  is the bit time. Typically  $BT$  is about 0.25. A correlation can be directly drawn between  $BT$  and the degradation from MSK. Premodulation low pass filters of other responses would also serve to limit bandpass bandwidth, but [Murota '81] illustrates that a Gaussian filter response is an excellent choice.

<sup>6</sup>A Gaussian filter's frequency and time domain responses have the same form.

<sup>7</sup>FSK with minimum tone spacing defines MSK.

<sup>8</sup>Built into this relationship is the assumption that the predetection channel has 'brickwall' bandpass response and bandwidth equal to the bit rate. However, the transceiver bandwidth is neither 'brickwall' nor has bandwidth equal to the bit rate. The 3 dB bandwidth of the transceiver used in the groundstation was measured to be 15 kHz, much greater than 9.6 kHz given by the bit rate of 9600 bps. The effects this are difficult to predict and the relationship given is a best case scenario.

<sup>9</sup>This relationship was derived for a different method of non-coherent detection than used in the ground station transceiver, but it was assumed that well designed non-coherent detectors have equivalent performance.

Figure 9 shows plots of coherently and non-coherently detected FSK as well as 2 dB degradations expected from gaussian filtering.

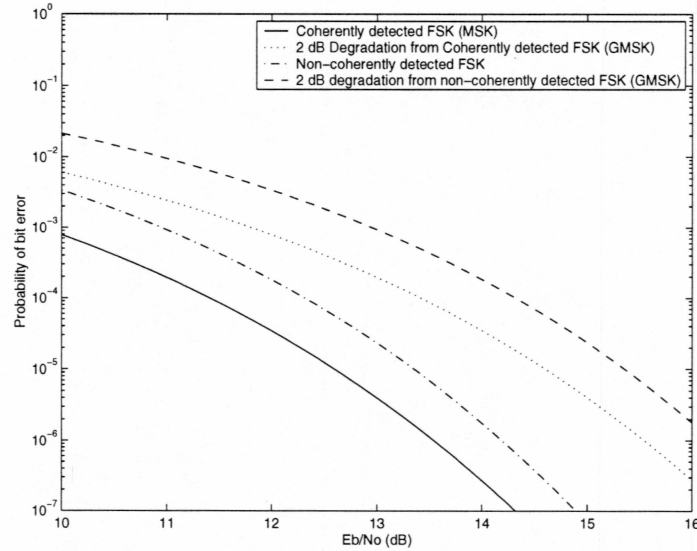


Figure 9: Error performance of MSK and GMSK, both coherently and non-coherently detected

Equation 3 is valid for noncoherently detected FSK, which is the case for the FM discriminators found in the spacecraft and ground station receivers. It follows that the required  $\frac{E_b}{N_o}$  for a given  $P_e$  for noncoherently detected FSK signals is

$$\frac{E_b}{N_o} = -2 \ln(2P_e) \quad (5)$$

and thus for GMSK,

$$\left( \frac{E_b}{N_o} \right)_{required_{GMSK}} = \frac{-2 \ln(2P_e)}{d_{MSK}} \quad (6)$$

This is the expression implemented in the link budget.

**Determining Received  $\frac{E_b}{N_o}$**  Values for  $E_b$  and  $N_o$  will vary throughout the communication system, however their ratio will not, as the definition of  $N_o$  is tailored for every point in the communication system to represent the amount of noise in the detected signal. It is convention to calculate  $\frac{E_b}{N_o}$  with respect to the output of the antenna terminals;  $E_b$  is the energy per information bit at this point and  $N_o$  is defined as the noise power density to include the noise the rest of the receiver system will add to the signal.

**Determining  $E_b$**  The received energy per bit of  $E_b$  is solely a function of received signal power and data rate. The relationship is

$$E_b = C \cdot T_b = \frac{C}{R_b} \quad (7)$$

where  $C$  is the received signal strength (Watts),  $T_b$  is the duration of one bit (seconds), and the data rate  $R_b$  is  $\frac{1}{T_b}$  (bits/second). The data rate for the CX-1 control communication system was set to a fixed value of 9600 bits per second, so that the only variable that affects  $E_b$  is the received carrier power  $C$ .

The received signal power  $C$  depends on three factors: Transmission (dBW)  $T$ , Propagation  $P$  (dB), and Receive  $R$  (dB). This may be expressed as

$$C = T + P + R \quad (8)$$

The Transmission factor  $T$  (dBW), also known as Effective Isotropic Radiated Power (EIRP), is the net effect of average transmitter power  $P_T$  (dBW), transmission line loss  $L_T$  (dB) from amplifier to antenna, antenna efficiency, which describes how much power the antenna wastes as heat, and antenna gain  $G_T$  (dB)<sup>10</sup>:

$$T = EIRP = P_T - L_T + G_T \quad (9)$$

The Propagation factor  $P$  (dB) is primarily due to free space loss  $L_P$ , or path loss:

$$L_P = \left( \frac{4\pi R}{\lambda} \right)^2 \quad (10)$$

where  $\lambda$  is the wavelength of the signal and  $R$  is the distance between the transmitter and receiver. The link budget was calculated in terms of elevation angle from the horizon to the spacecraft. This angle and the orbit height determine the slant range distance  $R$  as illustrated in Figure 10. The slant range can be expressed as

$$R = R_e \cos(\Phi) + \sqrt{R_e^2 \cos^2(\Phi) + 2R_e h + h^2} \quad (11)$$

<sup>10</sup>Antenna gain is directivity reduced by antenna efficiency, however wire antennas have a sufficiently high enough efficiency so that directivity and gain are used interchangeably.



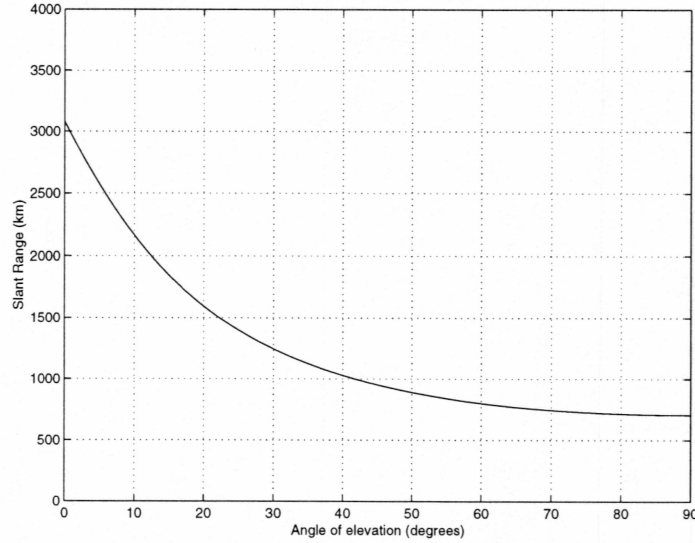


Figure 10: Illustration of slant range and angle of elevation for the CX-1 orbit

where  $R_e$ ,  $\Phi$ , and  $h$  are defined in Figure 11. Atmospheric absorption is negligible at VHF/UHF frequencies and was not considered in the link budget. Therefore,

$$P = L_P \quad (12)$$

Path loss for the two frequencies that will be used for CX-1 are plotted in Figure 12.

The Reception factor  $R$  (dB) is the receive antenna gain  $G_R$  (dB) less any polarization mismatch between the received signal and receive antenna  $\eta_{pol}$  (dB). For a steerable antenna, the estimated rms pointing error  $\eta_{pointing}$  (dB) may also detract from signal strength:

$$R = G_R - \eta_{pol} - \eta_{pointing} \quad (13)$$

Using the previous expressions, a value of  $E_b$  can be calculated from the data rate, satellite orbit, and characteristics of the transmitter and receiver.

**Determining  $N_o$**  The noise power spectral density  $N_o$  in the recovered signal may be related to the system noise temperature by

$$N_o = kT_{sys} \quad (14)$$



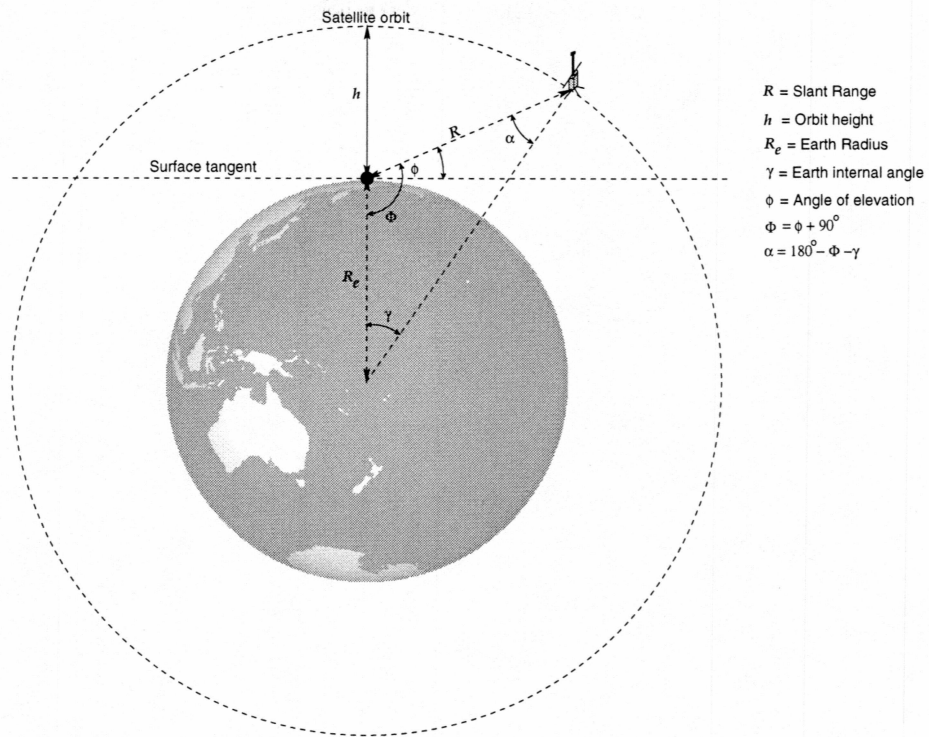


Figure 11: Illustration of slant range variables

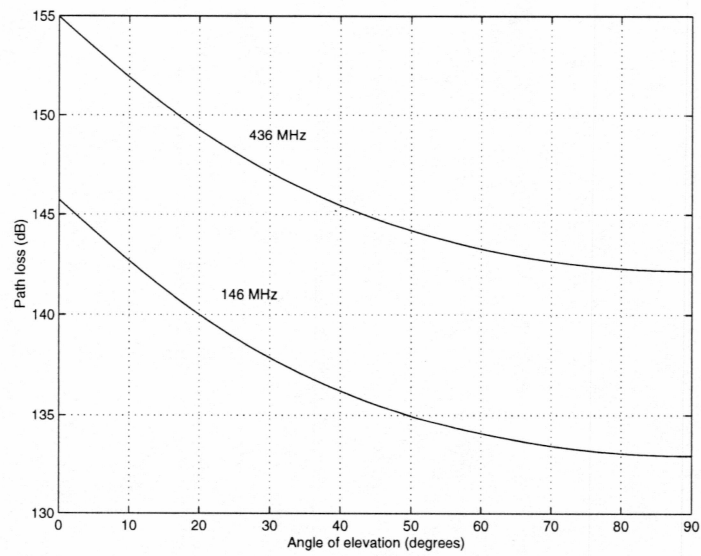


Figure 12: Path loss for the CX-1 signal links

where  $k$  is Boltzmann's constant and  $T_{sys}$  is the effective system temperature in Kelvin.  $T_{sys}$  has two contributors, the antenna noise temperature  $T_A$  and the effective receiver noise temperature  $T_R$ <sup>11</sup>:

$$T_{sys} = T_A + T_R \quad (15)$$

The antenna noise temperature is determined by how much black body radiation noise the antenna picks up from the ambient environment.

The receiver noise temperature describes how much noise the receiver adds to the signal. This can be calculated from the effective noise temperatures from all of the receiver elements such as transmission lines, preamplifiers, and the radio itself. In this context, 'receiver' refers to anything not including the antenna, since noise calculations are arbitrarily referred to the antenna terminals. See Figure 13 for clarity.

With reference to the antenna terminals, the receiver system temperature may be found as

$$T_R = T_1 + \frac{T_2}{G_1} + \frac{T_3}{G_1 G_2} \dots + \frac{T_i}{G_1 G_2 \dots G_{i-1}} \quad (16)$$

where the  $i^{th}$  element in the receive system has effective noise temperature  $T_i$  and signal gain  $G_i$ . For a lossy transmission line,

$$T_L = (L - 1) 290 \text{ K} \quad (17)$$

where  $L$  is  $\frac{1}{G_L}$ , the linear power loss of the line. Thus, transmission line loss adds noise to a detected signal.

A preamplifier is most often specified to have a certain noise figure, which can be related to the effective noise temperature by

$$T = (F - 1) 290 \text{ K} \quad (18)$$

where the noise figure  $F$  is defined to be the ratio of signal-to-noise-ratio out of a device to signal-to-noise-ratio into a device. This is a measure of extra noise added by the device.

If the receiver setup of Figure 13 is used,  $T_R$  can be expressed as:

<sup>11</sup>Note that  $T_R$  refers to the noise temperature of the entire receiving system, excluding antenna noise, while  $T_A$  refers only to the noise temperature of the receiver unit.

$$T_R = T_{L_1} + L_1 T_{LNA} + \frac{T_{L_2} L_1}{G_{LNA}} + \frac{T_r L_1 L_2}{G_{LNA}} \quad (19)$$

Thus, if antenna noise, cabling losses, preamplifier, and radio parameters are known, the noise power spectral density  $N_o$  can be calculated.

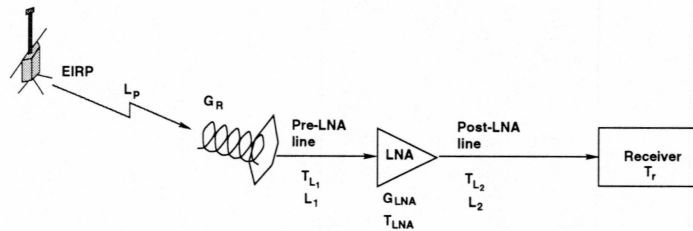


Figure 13: Illustration of receive system

Equation 16 implies that in order to add the least amount of noise to a detected signal, a low noise, high gain amplifier should be placed as close to the antenna terminals as possible. This is equivalent to saying that the “front end” of a receiving system is the most critical part, in terms of noise.

## Downlink Budget

The downlink budget is shown in Table I for various angles of elevation. A sample set of calculations may be found in Appendix C.

**Frequency:** The downlink frequency  $f$  is 436.75 MHz, which is in a band designated for amateur satellite communications.

**Wavelength:** The wavelength is calculated from the frequency as

$$\lambda = \frac{c}{f} \quad (20)$$

where  $c$  is the speed of light in vacuum ( $\frac{\text{m}}{\text{s}}$ ) and  $f$  is the frequency (Hz).

**Orbit Height:** The CX-1 Spacecraft will be in a low-eccentricity orbit (nearly round) with a nominal altitude above the earth of 706 km. The orbit height is used in Slant Range calculations, which determine Path Loss.

**Elevation Angle:** The slant range from the ground station to the satellite is a function of the elevation angle. Therefore, the link budget was calculated at several elevation angles.

## Satellite Transmit

**Power:** The CX-1 transmitter output power will be nominally 2 Watts.

**Line Loss:** The estimated signal loss from power amplifier to spacecraft transmit antenna.

**Antenna Gain:** The CX-1 spacecraft was gravity gradient stabilized so that the spacecraft remained vertically oriented with respect to its sub-satellite point. The transmit antenna was designed to be an omnidirectional antenna, but there will be some antenna pattern variation with different angles of elevation. As the spacecraft passed across the sky, the relative angle between a ground station's relative vertical direction and the spacecraft's vertical direction will vary. This is angle  $\alpha$  in Figure 11. As the angle  $\alpha$  varies throughout a pass, the antenna gain will vary. The University of Colorado provided a spacecraft transmit antenna pattern showing the effect of angular displacement from the spacecraft's nadir upon the transmit antenna pattern. Overall, the variation ranged from -3 to +3 dB. Hence, for low angles of

Table I: Downlink budget

Item	Symbol					
Frequency (MHz)	$f$	436.75				
Wavelength (cm)	$\lambda$	69				
Orbit height (km)	$h$	706				
Elevation angle (degrees)	$\Phi$	5°	25°	45°	65°	90°
<b>Satellite Transmit</b>						
Power (W)	$P_t$	2				
Power (dBW)	$P_{dB}$	3				
Antenna gain (dB)	$G_T$	-2	-1	2	3	3
Line loss (dB)	$L_T$	1				
EIRP (dBW)	$EIRP$	0	1	4	5	5
<b>Propagation</b>						
Slant range (km)	$R$	2600	1400	950	770	710
Path loss (dB)	$L_{dB}$	154	148	145	143	142
Total propagation loss (dB)	$P$	154	148	145	143	142
<b>Ground Station Receive</b>						
Antenna gain (dB)	$G_r$	17				
Pointing loss (dB)	$\eta_{pointing}$	-0.5				
Total reception gain (dB)	$R_z$	16.5				
Pre-LNA line loss (dB)	$L_{1dB}$	0.2				
Pre-LNA line loss noise temperature (K)	$T_{L1}$	14				
LNA noise figure (dB)	$F_{LNA,dB}$	1				
LNA noise temperature (K)	$T_{LNA}$	75				
LNA gain (dB)	$G_{LNA}$	16				
Post-LNA line loss (dB)	$L_{2dB}$	5				
Post-LNA line loss noise temperature (K)	$T_{L2}$	627				
Receiver noise temperature (K)	$T_r$	2610				
Net receiver noise temperature (K)	$T_R$	326				
Antenna noise temperature (K)	$T_A$	130	70	70	70	70
System noise temperature	$T_{sys}$	456	396	396	396	396
Received noise power density (dBW/Hz)	$N_o$	-202	-203	-203	-203	-203
Received signal power	$C$	-137	-131	-124	-122	-121
$\frac{G_r}{T_{sys}}$ (dB/K)		-10				
Receiver input level ( $\mu V$ )		4	7	15	21	23
<b>Digital</b>						
Data rate (bps/dBbps)	$R/R_{dB}$	9600/40				
Received $\frac{C}{N_o}$ (dBHz)	$\frac{C}{N_o}$	65	71	78	81	81
Received $\frac{E_b}{N_o}$ (dB)	$\left(\frac{E_b}{N_o}\right)_{received}$	25	32	38	41	42
Maximum allowed BER due to noise	$P_r$	$1 \times 10^{-7}$				
$\frac{E_b}{N_o}$ Required	$\left(\frac{E_b}{N_o}\right)_{required}$	17				
Implementation guess (dB)		-3				
Noise BER Margin		5	12	18	21	22

elevation, the transmit antenna gain was about -2 dB. This information was garnered from an antenna radiation pattern simulation from the University of Colorado. This is represented in Figure 14.

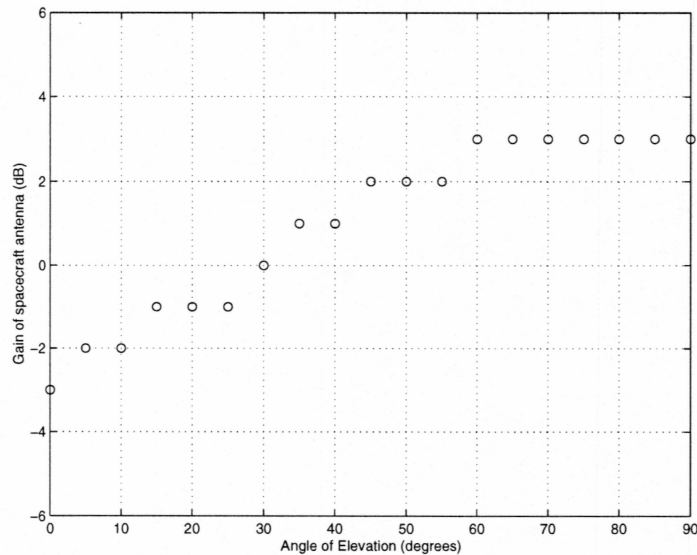


Figure 14: Spacecraft transmit antenna gain as a function of elevation angle

**EIRP:** Effective Isotropic Radiated Power. (Equation: 9)

### Propagation

**Slant Range:** The direct distance to the satellite. (Equation: 11)

**Path Loss:** Signal strength loss due to transmission through free space. (Equation: 10)

**Atmospheric Absorption:** The effect of the atmosphere is negligible at VHF/UHF frequencies.

**Total Propagation Loss:** The net propagation loss is equal to the path loss in this link budget. (Equation: 12)

### Ground Station Receive

**Antenna Gain:** The 436 MHz helical receive antenna was measured to have a maximum gain of 17 dBi.



**Pointing Loss:** The antenna steering system can point the antennas to within  $\pm 5^\circ$  of the intended direction. This is estimated to correspond with a maximum signal loss of 0.5 dB.

**Total Reception Gain:** The net effect of the items in the receive section of the link budget. The total reception gain relates how much signal strength is available at the receiving antenna terminals for a given field strength incident upon the antenna. (Equation 13)

**Pre-LNA line loss:** This is the attenuation of the short cable running from the antenna terminals to the low noise preamplifier. The preamplifier was mounted directly on the antenna to minimize this loss. The cable was 20 cm of Belden 9913F coaxial cable with N-connectors whose insertion loss was measured to be 0.2 dB.

**Pre-LNA line loss noise temperature:** This figure is the Pre-LNA line loss converted to an equivalent noise temperature for use in calculating the system noise temperature. Since this is the first term in the equation for  $T_{sys}$ , it can have a significant impact upon  $T_{sys}$  and should therefore be minimized. (Equation 17)

**LNA Noise Figure:** The low noise preamplifier used was specified to have a noise figure of 1 dB. This was an Advanced Receiver Research (ARR) model MSP432VDG.

**LNA Noise Temperature:** The LNA noise figure converted to an equivalent noise temperature. (Equation 18)

**LNA Gain:** The ARR MSP432VDG LNA is specified to have a gain of 16 dB.

**Post LNA Line Loss:** About 30 m of Belden 9913F coaxial cable was used and the insertion loss was measured to be 5 dB at 435 MHz.

**Post LNA Line Loss Noise Temperature:** The post LNA line loss converted to an equivalent noise temperature. (Equation 17)

**Receiver Noise Figure:** This is  $T_r$  and refers to the ground station radio, and ICOM 821H. An upper limit of its noise figure was measured to be about 10 dB. The method used to measure this is explained in Appendix B.

**Receiver Noise Temperature:** This is the receiver noise figure converted to an equivalent noise temperature. (Equation 18)

**Net Receiver Noise Temperature:** This is  $T_R$  and refers to the net noise contribution of everything following the antenna terminals. (Equation 19)

**Antenna Noise Temperature:**  $T_A$  reflects the amount of noise added to the signal by the antenna and is a function of brightness temperature in the antenna pattern. This has two contributors, the black body radiation of the sky and Earth. Though the ground station receiving antenna was always pointed at the sky, earth thermal noise contributed to the antenna noise temperature at low angles of elevation and through sidelobes of the antenna. The effective thermal noise temperature of the earth was assumed to be 290 K and the black body contribution from the sky corresponds to about 70 K [Sklar '88]. When the antenna was pointed at the horizon, the earth and sky equally occupied the antenna pattern, so the effective antenna noise temperature was the average of Earth and sky noise temperatures in this case.

It is also possible for the sun to transit the antenna beam and cause the antenna temperature to rise high enough to obliterate communications. However, the sun will be in the main beam of the receiving antenna about 6% of the time on average, which is low enough to neglect.

**System Noise Temperature:** The system noise temperature  $T_{sys}$  is the final figure of how much noise is added to the received signal. (Equation 15)

**Received Noise Density:** (Equation 14)

**Received Signal Power:** This is the signal power available from the antenna terminals.

$\frac{G_r}{T_{sys}}$ : This is a figure of merit for a ground station in general.  $G_r/T_{sys}$  illustrates the combined effect of the ground station's receiving antenna and the receiver noise characteristics. This is included for completeness, but does not have any direct bearing upon the link margin.

**Receiver Input Level:** Commonly, a receiver manufacturer specifies 'receiver sensitivity', an input level that gives satisfactory performance with typical input noise levels. This has been included here as a check against the specified sensitivity, which is  $0.2 \mu V$  for the ICOM 821H transceiver used. The voltages given in this entry are obtained from the receiver input power and the transmission line impedance,  $50 \Omega$ .

**Data Rate:** The data rate for control communications was given to be 9600 bits per second.

**Receive  $\frac{C}{N_o}$ :** This is the received signal power level  $C$  divided by noise power density  $N_o$ , which is a stepping stone for calculating  $\frac{E_b}{N_o}$  in the received signal.

**Required  $\frac{E_b}{N_o}$ :** Energy per bit to noise power density ratio is found by dividing  $\frac{C}{N_o}$  by the data rate.

**Maximum BER:** This is the desired value given for satisfactory communication and is used to calculate the necessary  $\frac{E_b}{N_o}$  to achieve this. The protocol used in communication should still be functional when used in a link with this value of Maximum BER. For TCP, a BER of  $1 \times 10^{-7}$  reduces the effective data rate to about 85% of the error-free data rate [Ernst '96]. Higher bit error rates begin to seriously erode TCP performance.

**$\frac{E_b}{N_o}$  Received:** This is the value necessary to achieve the desired bit error rate. (Equation 6)

**Implementation Guess:** This value is included to compensate effects that have not been properly accounted, such as in Equation 4. In this case, the bandpass response of the ground station transceiver did not match the conditions under which Equation 4 was derived.

**Noise BER Margin:** This value would represent the amount of signal power that is available in excess of that required for communications at or below the maximum BER due to noise specified.

Overall, the downlink budget indicates that the BER due to noise will be easily less than  $1 \times 10^{-7}$ , as indicated by positive margin values.

## Uplink Budget

For comparison, the uplink budget is shown in Table II. The downlink budget is developed a little more extensively than the uplink budget: the effects of a preamplifier and line losses are readily calculated in the downlink budget. Most of the entries in the uplink budget are analogous to those in the downlink budget, however a few entries warrant further discussion:

**Satellite Receive Antenna Gain:** The spacecraft's receiving antenna will be a linear dipole that has a maximum gain of about 1.5 dBi.

Table II: Uplink budget

Item	Symbol					
Frequency (MHz)	$f$	145.86				
Wavelength (m)	$\lambda$	2.06				
Orbit height (km)	$h$	706				
Elevation Angle	$\Phi$	5°	25°	45°	65°	90°
<b>Ground Station Transmit</b>	T					
Power (W)	P	25				
Power (dBW)	P	14				
Pointing Loss (dB)		-0.5				
Antenna gain (dBi)	$G_T$	9				
Line loss (dB)	$L$	3				
EIRP (dBW)		19.5				
<b>Propagation</b>	P					
Slant range (km)	$R$	2600	1400	950	770	710
Path loss (dB)	$L_p$	-144	-139	-135	-134	-133
Absorption (dB)		0				
Total propagation loss (dB)		-144	-139	-135	-134	-133
<b>Satellite Receive</b>						
Antenna gain (dBi)	$G_r$	1.5				
Pointing loss (dB)		-2.5				
Polarization mismatch (dB)		-3.0				
Total Reception Gain (dB)		-4.0				
Net receiver noise temperature (K)	$T_R$	900				
Antenna noise temperature (K)	$T_A$	150				
System noise temperature (K)	$T_{sys}$	1050				
Received noise power density (dBW/Hz)	$N_o$	-198				
Received signal power (dBW)		-129	-123	-120	-118	-117
Receiver input level (dBm)		-99	-93	-90	-88	-87
<b>Digital</b>						
Data rate (bps/dBbps)		9600/40				
Received $\frac{C}{N_o}$ (dBW/Hz)	$\frac{C}{N_o}$	70	75	79	80	81
Received $\frac{E_b}{N_o}$ (dB)	$\frac{E_b}{N_o}$	30	35	39	41	41
Maximum allowed BER due to noise	$P_e$	$1 \times 10^{-7}$				
$\frac{E_b}{N_o}$ Required (dB)	$\frac{E_b}{N_o}$	17				
Implementation guess (dB)		-3.0				
Noise BER Margin (dB)		10	16	19	21	21

**Satellite Receive Pointing Loss:** The orientation of the spacecraft with respect to the ground station is expected to be unknown and variable through the pass. The result is that the spacecraft's receiving antenna gain is expected to fluctuate between null and maximum gain, with an estimated average 'pointing loss' of 2.5 dB.

**Net Receiver Noise Temperature:** This is expected to be about 900 K, based upon discussions with the manufacturer of the receiver, SpaceQuest.

### 3.2.2 Probability of Error due to Intersymbol Interference and Nonlinear Channel Effects

Intersymbol interference (ISI) occurs when the channel response of the link does not properly accommodate the signal being passed through it. Insufficient bandwidth and/or improper channel filtering will lead to ISI. For a given symbol rate, there is a theoretical minimum bandwidth that must be available to avoid intersymbol interference. Even if sufficient bandwidth is available, the channel frequency response must be equalized to avoid ISI [Pratt '86]. Deviation from the appropriate frequency response will give rise to intersymbol interference.

The probability of bit error due to intersymbol interference is much more difficult to predict than the effect of Gaussian noise upon the system. Figure 15 shows baseband channel measurements from one amateur transceiver to another. This was measured by using an audio signal generator applied to the input of one transceiver and observing the received signal amplitude from the other transceiver with an rms voltmeter. Ideally, this would be a completely flat response. GMSK requires low frequency response to DC for operation without ISI [Pacomm '94]. The channel response exhibits tapering performance with lower frequencies, and this contributes to intersymbol interference.

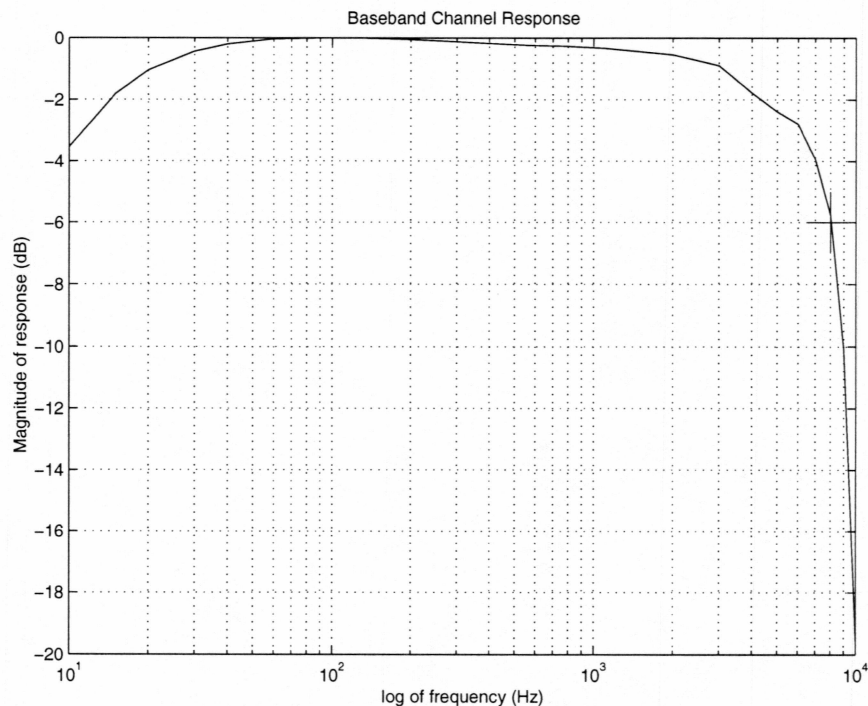


Figure 15: Baseband transceiver channel response.



To reduce ISI, channel filters could have been fabricated to flatten the response shown in Figure 15, or modem filtering could have been tailored to achieve the same effect.

The channel response across the link, from modulator to detector, had some amount of nonlinearity, which gives rise to distortion and intermodulation products. The effect of nonlinearity and intersymbol interference combine to yield a bit error probability due to the equipment characteristics. This is very difficult to predict and was therefore measured instead. To make this measurement, signal strength was set to a value that assured that noise was negligible: the receivers indicated maximum signal strength. It was found that the bit error probability due to intersymbol interference and channel nonlinearities was about  $6 \times 10^{-9}$ , as described in Appendix A.

### 3.2.3 Probability of Error due to External Interference

Since communications with CX-1 from the Alaska ground station will be in the amateur bands in a sparsely populated area, external interference is not expected to be a factor in the net probability of bit error.

## 3.3 Remarks

The link budget may easily be misinterpreted. Short slant ranges, and therefore greater received signal strengths, yield a greater noise BER margin. This may easily be confused with the overall BER, which has other contributors that define the minimum BER. In the case of the Citizen Explorer project, the BER had a lower limit of about  $6 \times 10^{-9}$  due to ISI and nonlinear effects which could only be worsened by noise. Positive margins in the link budget indicate the BER of the link with CX-1 will be limited not by noise, but by the equipment imposed BER due to ISI and nonlinear effects.

A constricting bandwidth, or improperly equalized channel, would certainly introduce errors; however, this would be independent of received signal strength, and thus are not part of the link budgets of Tables I and II.

## 4 Antennas

This section describes the antenna requirements for the ground station, how the requirements were satisfied, and the antenna design and testing.

Consideration of the link budgets was the first step in determining the antenna requirements for the link budgets. A key decision about the antenna type was in regards to antenna steering. Fixed antennas without an active steering system would have been preferred as this would simplify the ground station operation. Non-directional antennas by definition have little or no gain, so the effect of using unity gain antennas was studied in the link budgets. The uplink budget revealed that an omnidirectional antenna with circular polarization, namely a quadrifilar helical antenna, would satisfy margin requirements. However, the downlink budget clearly indicated a need for a directional antenna. Since the downlink budget mandated a directional, steerable antenna, a directional antenna was made for the uplink as well: the work of implementing an antenna steering system was already mandated.

The link budgets were examined to determine the required directivity for each antenna. The downlink needed a healthy boost, so 15 dBi was chosen. The uplink was not as limited and more transmit power was available at the groundstation in comparison to the spacecraft. The uplink antenna was built for a gain of 10 dBi, arbitrarily limited by the size of the boom available

The uplink antenna was chosen to be circularly polarized because the spacecraft's receive antenna will be linear whip antenna. The relative orientation of the spacecraft's receiving antenna would have been very difficult to measure or predict, so circular polarization was used on the uplink to avoid deep fades due to polarization mismatch. This compromise results in a constant 3 dB loss in the link by receiving the ground station's circularly polarized transmissions with the spacecraft's linearly polarized antenna.

Since the spacecraft's transmitting antenna was left hand circularly polarized, it follows that the ground station receiving antenna was also left hand circularly polarized.

### 4.1 Antenna Design

The antennas used to fill the directivity and polarization requirements were axial-mode monofilar helical antennas [Kraus '88]. These antennas were mounted side-by-side on a steerable boom as

shown in Figure 16. Helical antennas have wide bandwidth, are easy to match to  $50 \Omega$  transmission line, and are forgiving in their construction. An axial mode helical antenna is a traveling wave antenna. The geometry of the helixes yields an increased-directivity condition.

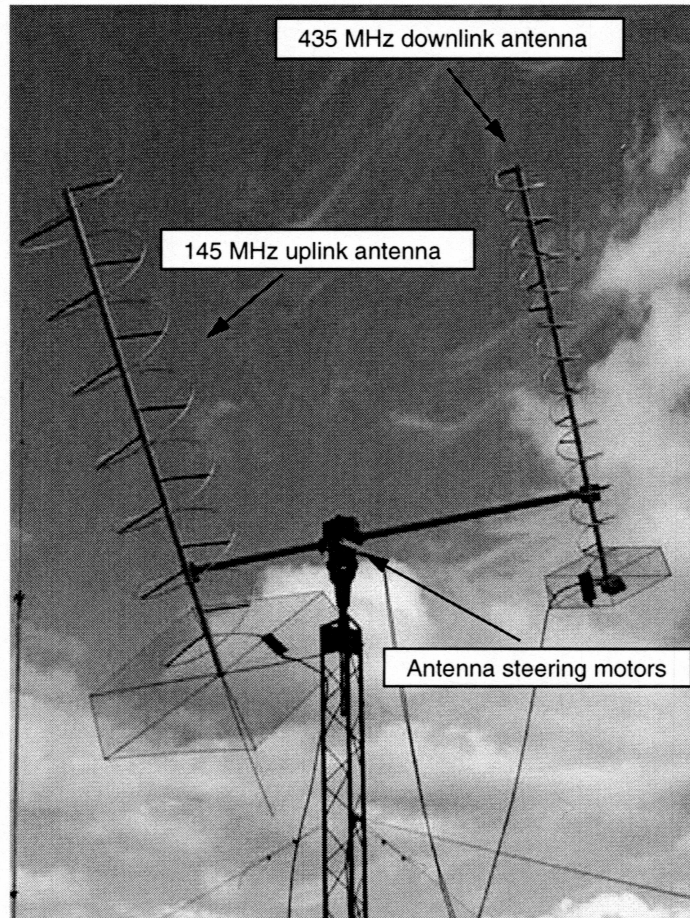


Figure 16: Photograph of antennas

The geometry of the helix was easily determined by applying the guidelines given in [Kraus '88]. Figure 17 shows the design parameters of the axial mode monofilar helical antenna. The parameters shown are the pitch angle of the helix ( $\alpha$ ), the helix coil spacing in terms of wavelengths ( $S_\lambda$ ), and the helix circumference in terms of wavelengths ( $C_\lambda$ ), where  $\lambda$  is the free space wavelength at the design center frequency. The length of the antennas is determined by the number of turns ( $n$ ) and the coil spacing ( $S$ ).

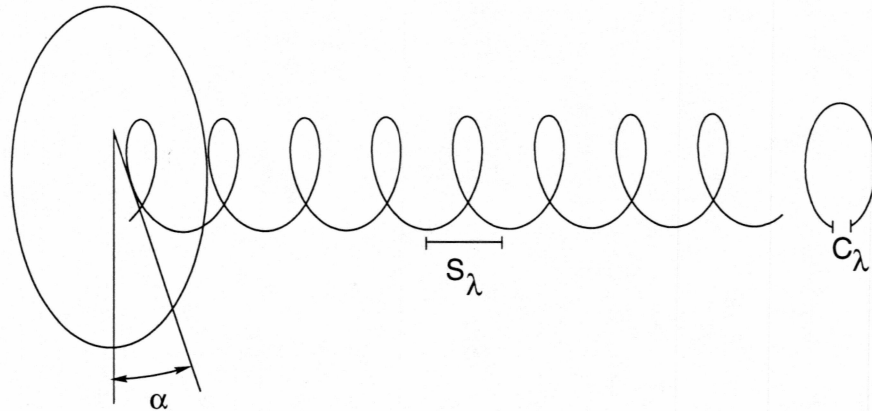


Figure 17: Diagram of helical antenna

Provided that the following criteria are met

$$0.8 < C_\lambda < 1.15 \quad \text{and} \quad 12^\circ < \alpha < 14^\circ \quad (21)$$

the directivity ( $D$ ) and Half Power Beam Width (HPBW) of the antenna can be approximated as [Kraus '88]

$$D = 12C_\lambda^2 n S_\lambda \quad (22)$$

$$HPBW = \frac{52^\circ}{C_\lambda \sqrt{n S_\lambda}} \quad (23)$$

The ground plane shown in Figure 17 is present to increase the front-to-back radiation ratio and hence improve the beam efficiency of the antenna. The diameter of the ground plane is generally on the order of a wavelength. Table III summarizes the values used in the construction of each antenna.

For both antennas, the transition from coaxial transmission line to helical element was accomplished with a gradual transition from microstrip transmission line to free-floating element, as shown in Figures 18 and 19. The dielectric rectangle material is Delrin<sup>TM</sup>. Aluminum tubing was used for most of the helix, but the transition to microstrip line used copper tubing for malleability and solder-ability. The junction between the aluminum tubing and the copper tubing was reinforced with a brass bushing (inside) and the whole joint was sealed with conductive epoxy cement.

Both of the helices were wound about metallic booms. The metal boom tubing did not signifi-

Table III: Antenna parameters

Parameter	Symbol	2 m antenna	70 cm antenna
Helix circumference (wavelengths)	$C_\lambda$	0.8	1.0
Helix spacing (wavelengths)	$S_\lambda$	0.213	0.231
Pitch angle	$\alpha$	12°	13°
Directivity	$D$	10 dBi	15 dBi
Number of turns	$n$	7	12
Diameter of helix		53 cm	22 cm
Length of helix		2.5 m	1.9 m
Ground plane diameter		1.8 m	0.7 m

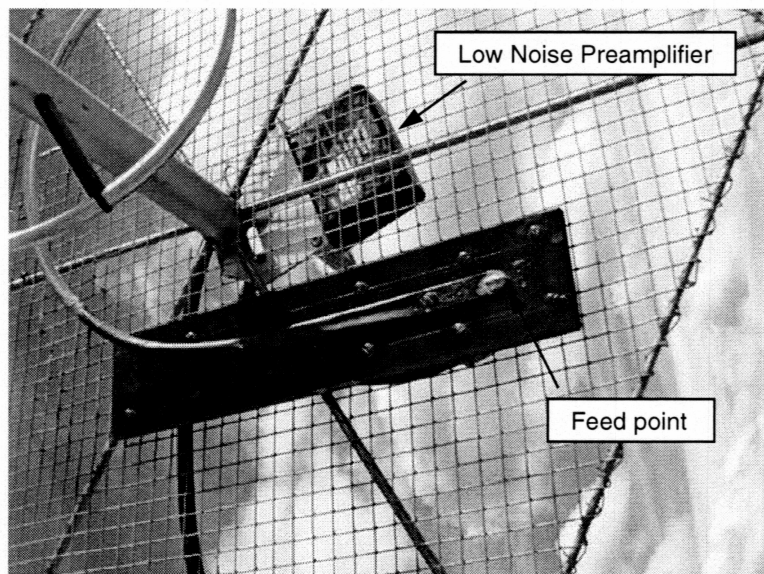


Figure 18: Top view of 435 MHz antenna base



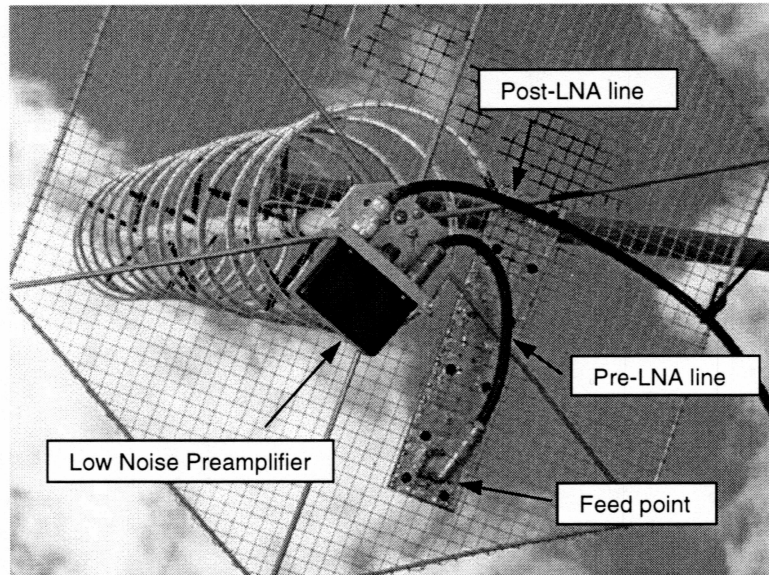


Figure 19: Bottom view 435 MHz antenna base

cantly affect the radiating fields within the helix, as the fields are transverse to the boom. However, the supports for the helices had to be made from a non-conductive material since they lay parallel to the electric fields within the helices. Similarly, the material chosen for the cross-boom was fiberglass.

## 4.2 Antenna Steering

An off-the-shelf system was employed to steer the antennas. This was a Yeasu-5400B antenna motor kit produced for amateur radio applications. The kit included two motors, one for azimuth steering and one for elevation steering, and a relay box that turned the motors on and off. Within each motor housing was a potentiometer that was used for position feedback. The motors did not have a variable speed control, but were switched on and off with relays. The motors were switched on until the desired position was reached and then switched off. This did not provide for very smooth movement, especially when combined with the large moment-arms of the antennas mounted on a cross-boom, as shown in Figure 16. In addition, the fiber-glass cross-boom could store a significant amount of mechanical energy, which decreased the damping of the antenna structure. To worsen the matter, one of the motors (the azimuth motor) had several degrees of play, attributed to backlash in the internal gear train, where the internal brake was ineffective. The net result was that the antenna structure was underdamped in the azimuthal plane. Oscillations of about  $\pm 3^\circ$

were observed. However, the beam widths of the antennas were sufficiently wide so that the stray movements of the antenna structure had no noticeable effects upon signal levels.

### 4.3 Antenna Testing

Once the antennas were constructed, return loss and patterns were measured to check proper operation. In order to verify the directivity of the antennas, antenna pattern measurements were taken in the horizontal plane. The axial ratio of these helical antennas was assumed to be near unity so that the same pattern would be expected from the vertical plane. Figures 20 and 21 show the pattern data in polar form. From these data, the Half Power Beam Widths (HPBW) can be determined.

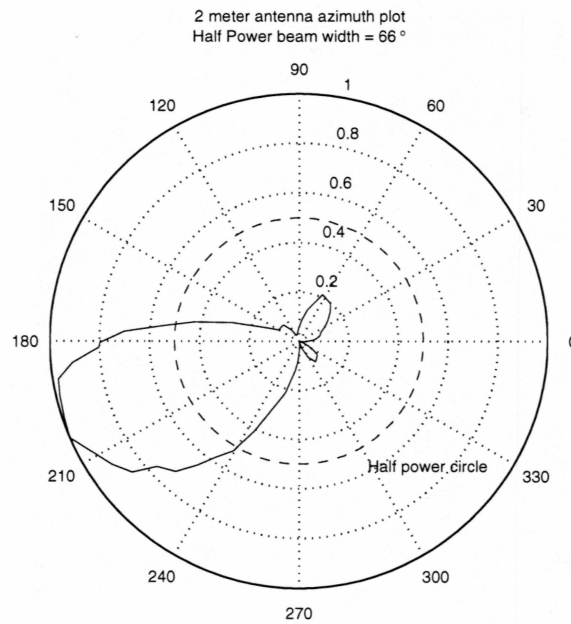


Figure 20: Azimuth plot of 145 MHz helical antenna data

For a directional antenna, a relationship between the HPBW and the directivity of the antenna can be determined from Equations 22 and 23:

$$D = \frac{32450}{HPBW^2} \quad (24)$$

Thus, if the Half Power Beam Width is known from measurements, the antenna directivity can be deduced<sup>12</sup>. With this data, the antenna directivities were determined to be about 9 dBi and 17 dBi for the uplink and downlink antennas, respectively, which were near the design values.

<sup>12</sup>In a separate context, [Kraus '88] derives  $D \cong \frac{41000}{HPBW^2}$ , which is about 1 dB greater than Equation 24.

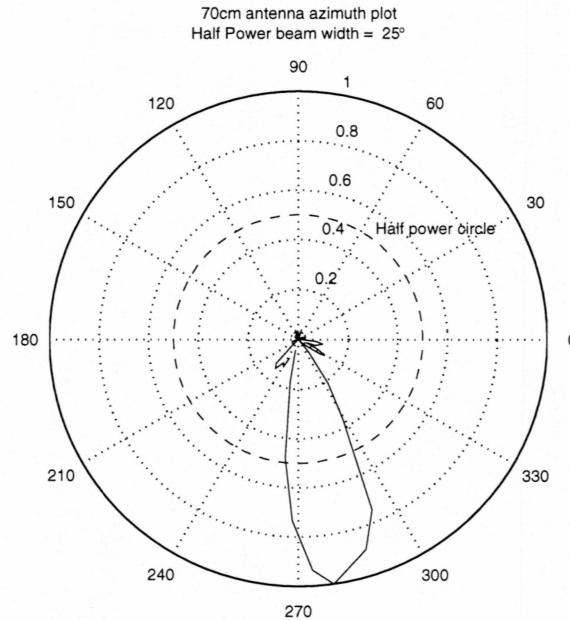


Figure 21: Azimuth plot of 435 MHz helical antenna data

In testing an antenna, it is also important to observe the return loss at the antenna terminals. For a one port network, such as an antenna in an anechoic field, the return loss is identical to the power reflection coefficient. If the antenna is a good match to the transmission line, the return loss will be high, and little power will be reflected from the antenna. A rule of thumb for a functional antenna is that the return loss should be at least 10 dB, or that less than 10% of the power is reflected from the antenna terminals.

A high return loss indicates that the antenna is absorbing RF power, but does not indicate in any fashion how it is dissipating that power. Some fraction will be dissipated as heat while the rest will propagate as propagating waves. However, a reasonable return loss is good assurance that the antenna is working properly if a proven antenna geometry is used.

The return losses of the ground station antennas were measured with a network analyzer and the results are shown in Figure 22 and 23. The 145 MHz antenna had a return loss of about 13 dB, while the 445 MHz antenna had a return loss of about 15 dB at their operating frequencies. This indicates that the antennas reasonably matched the transmission lines.

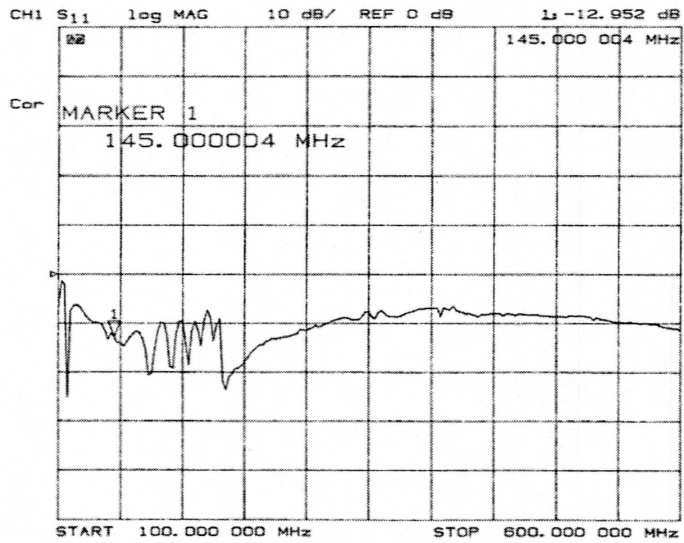


Figure 22: Return loss measurements of 145 MHz antenna

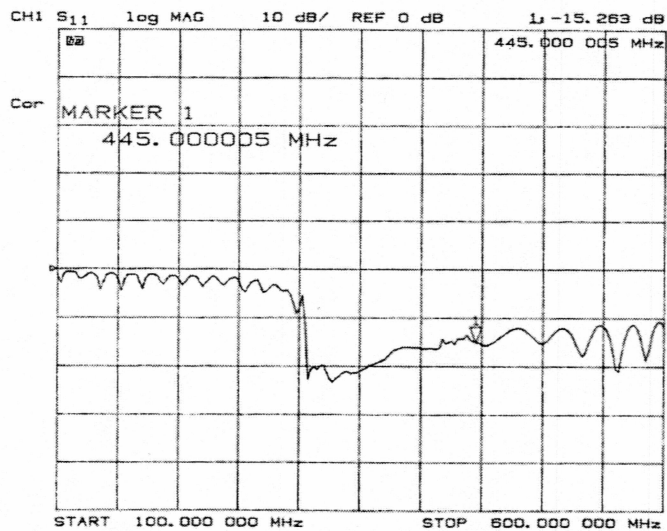


Figure 23: Return loss measurements of 445 MHz antenna



## 5 Ground Station Testing

A complete test of the Citizen Explorer ground station consisted of two parts:

1. Testing the tracking system and RF communication link
2. Testing a network interface via transceivers

### 5.1 Testing the Tracking System

The components of the tracking system were tested in a number of ways. The following is a description of the test of each component of the tracking system.

**Timekeeping** The 'ntpd' (network time protocol daemon) program that was used to maintain the ground station clock runs continuously and can be checked with a query program 'ntpq' which shows how the system clock is corrected for drift as well as statistical timeserver information. The UAF timeserver is referenced to GPS satellite clock signals, which have atomic clocks on board. The GPS satellite clocks themselves are maintained by a ground based master control station clock.

**Two line element updates** When the SatTrack program is started, it displays when the orbital elements were created, which provides a means to check the currency of the information. In addition, if the regularly scheduled download is not successful, the ground station computer root account is notified via email that there was an error.

**Transceiver frequency tracking** When receiving frequency updates from SatTrack via a serial port, the LCD of the ground station's transceiver shows activity with every update. Most importantly, the displayed uplink and downlink frequencies are continuously changing. The accuracy of the Doppler-shifted frequencies was verified with successful tracking of existing amateur spacecraft. Correction for Doppler shift for both uplink and downlink is only performed at the ground station.

**Antenna Steering** Accuracy of the antenna steering mechanisms are checked by monitoring the readouts on the antenna relay box. The readouts are galvanometers which interpret antenna positioning from the voltage returned by the internal potentiometers within the antenna motors. Further verification of positioning is gained by using SatTrack to track the Sun or the

Moon. If the sky is clear, the alignment of the antennas is easily verified with the antennas' shadows or by observing from the back end of the antennas. Accuracy is easily seen to be within  $\pm 3^\circ$  with this method. Once again, successful tracking of existing amateur satellites illustrated that positioning of the antennas was functional.

**Antenna Performance** Antenna directivity and matching quality were measured as previously described in Section 4.3. The fact that the antennas functioned as expected with existing amateur spacecraft gave further proof that they performed acceptably. Antenna gain could not be readily verified with existing spacecraft, as information about their transmitting power and antenna patterns is not readily available.

## 5.2 Testing the Network Interface

In order to test the functionality of establishing a TCP/IP/PPP link via radio communications equipment, a pseudo-satellite was set up to emulate the CX-1 spacecraft. In terms of hardware, the pseudo-satellite consisted of an older i486 computer with a Linux operating system installed. The computer was accompanied by a set of packet controller/modems and a set of transceivers. In terms of software, a dummy version of the flight software will be developed at the University of Colorado to emulate the spacecraft. Although this software has not been delivered at the time of this writing, the setup can be used to establish a PPP link between the ground station and the pseudo-satellite.

Establishing a PPP link was done in three tiers, each successively involving more hardware. Figure 24 illustrates this approach. The first tier test involved establishing a PPP link using only

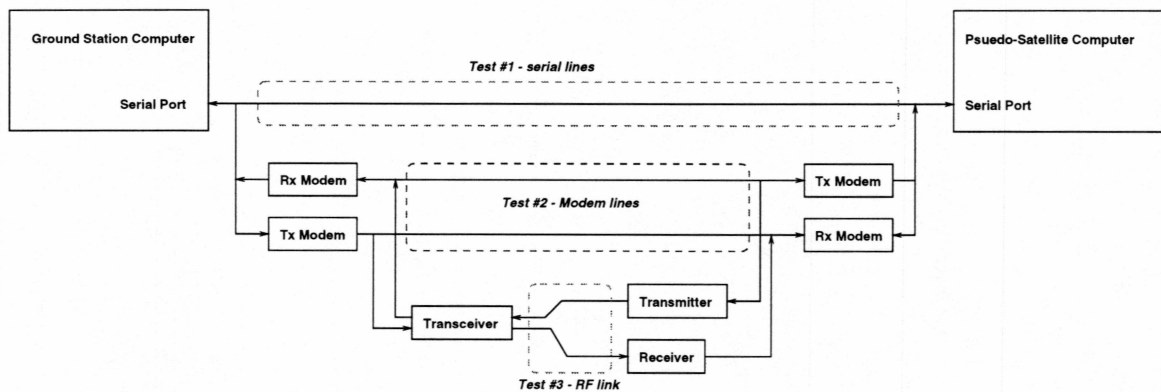


Figure 24: Testing the network interface in tiers

the serial ports of the two computers and a null modem serial cable<sup>13</sup>. This was done to verify that the PPP program was configured correctly and also to test the effective data rate of the network interface. It was found that data could be transferred in one direction at about 8000 bits per second, where the serial port speeds had been set to 9600 bps. This data rate was measured using the TCP application, 'ftp', to transfer a file from one machine to the other. The program reports the effective data rate when the transfer is complete. The apparent discrepancy between 8000 and 9600 bps is due to both TCP and PPP overhead. No convenient method of estimating the BER of this link was available; large files could be transferred with no loss of packets to generate BER data. Therefore, the BER of the serial port link was considered negligible.

The second tier test included the packet controller/modems. With the inclusion of these, the

<sup>13</sup>A null modem cable has the Tx, Rx, and handshaking signals swapped at one end

expectation is that the link in this case would have a slower effective data rate and some appreciable BER due to intersymbol interference. This was confirmed with an effective data rate of about 450 bps and BER<sup>14</sup> of  $6 \times 10^{-9}$  (99.999 packet success rate). Therefore, the added delay of AX.25 framing seemed to have severely hampered TCP.

The third tier test represented the most complete systems test available short of communicating with the spacecraft. The ground station transceiver was included as well as a transmitter and receiver for the pseudo-satellite. A single transceiver was not used in the pseudo-satellite setup because a low priced transceiver was not available that would operate in 9600 bps packet mode on both the 2 meter and 70 cm amateur bands at the same time. It was more economical to dedicate less costly transceivers to receive and transmit paths than to purchase another transceiver identical to that used in the ground station.

In addition, performing this test made apparent the necessity for separate packet controller/modems for receive and transmit functions. According to the manufacturer, each packet controller/modem can operate in full duplex, meaning that a single unit should be able to send and receive data simultaneously, suggesting that only one unit would be necessary. However, the manufacturer did not test these products in the manner that they were employed in this test, which was manifested by a data loss problem when a packet controller/modem in the transparent mode was receiving continuous data and transmitting continuous data. Most likely, the manufacturer used sporadic full duplex traffic instead of continuous. The effect was that the packet controller/modems only operated properly when used in half-duplex or simplex fashion. Since there is a separate frequency for uplink and downlink, there is no need to use half-duplex communication. The packet controller/modems were inexpensive enough to warrant the purchase of additional units so that each could be dedicated to simplex and would not produce unwarranted data loss.

Not shown in Figure 24 are serial line switching devices that were employed to facilitate testing with the packet controller/modems. In normal operation, the transmit, receive, and handshaking lines are shared between the transmit and receive packet controller/modems. However, to communicate with a single packet controller/modem for setup or diagnosis required that all the serial lines be directed to that particular unit. This was first done with cable-swapping, which was inconvenient. An electronic switching device was subsequently designed to handle this task much more conve-

---

<sup>14</sup>The measurement of BER is described in Appendix A

niently. The state of the serial line switching box was controlled via the parallel port. A simple C-program was used to set the appropriate state of the parallel port data signals. A simple graphical interface for this was assembled with the Qt interface for C/C++, which is shown in Figure 25.

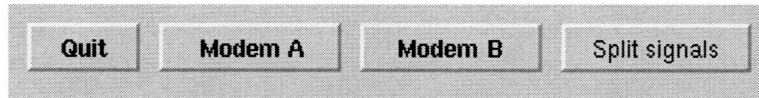


Figure 25: Graphical interface for serial line switcher

The link between transceivers of the ground station and pseudo-satellite was not direct, as shown in Figure 24, but was a free space propagation path. At first, the ground station and pseudo-satellite were in the same room with dummy loads attached to the transceivers. Stray fields provided sufficient coupling between transceivers to simulate reasonable signal strengths. When the functionality was proven, the ground station was moved to its final location several blocks away and connected to the helical antennas. Antennas were assembled at the site of the pseudo-satellite and the network interface was tested over the distance of about 1 kilometer.

The third tier test produced some illuminating results. Transferring binary files back and forth between the machines revealed that one direction of link performed significantly poorer than the other. The BER in transmitting from ground station to pseudo-satellite was about  $1.5 \times 10^{-7}$  (packet loss rate  $\approx 0.04\%$ ) which seemed acceptable. In the other direction, the BER from pseudo-satellite to ground station was  $8 \times 10^{-5}$  (packet loss rate  $\approx 18\%$ )<sup>15</sup>. The reason for this was suspected to be mediocre performance of the mobile transceiver that the pseudo-satellite was using to transmit. This suspicion was supported when baseband frequency responses of the transceivers were measured, as shown in Figure 26. The resulting poor performance was sufficient to cripple any TCP applications that were launched on this link. When timeouts did not kill the ftp application, it returned transfer rates of a dismal 8 bps.

This test showed that the same version of TCP that does well with the ethernet is not acceptable for the test-link. TCP is most commonly deployed on multi-user networks, where packet losses are due to congestion (packet collisions). One remedy to congestion is to reduce the rate at which data is transmitted [Comer '99].

However, in the test RF link, there was no congestion, and the packet loss was due to corruption

---

<sup>15</sup>Packet size was about 2500 bits



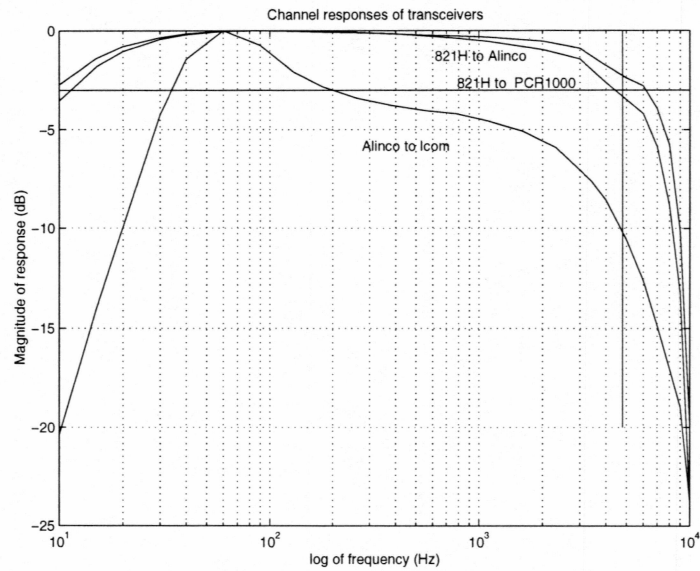


Figure 26: Baseband frequency response of transceivers .

and noise. The remedy that TCP applied was precisely opposite of the proper action: immediate retransmission of data. In order to obtain acceptable performance TCP will have to be tuned specifically for the RF link. Extensive research has been conducted in how to optimize TCP for satellite links [Allman '97]. The key results are that larger TCP windows should be used, as well as modifications to 'slow start' and congestion avoidance algorithms.

The critical decoder on the spacecraft, which will have the function of a packet controller in transparent mode, is expected to perform much better than the mobile transceivers used in the pseudo-satellite, as it was custom designed/manufactured for CX-1. In addition, the modem part of the spacecraft's communication system was commercially produced by an aerospace communications company. Therefore, TCP is expected to perform acceptably in the actual spacecraft-ground station link.

## 6 Equipment Description

This section outlines the equipment employed in the Citizen Explorer Alaska Ground Station. The function of the equipment in relation to the rest of the station is explained as well as more detailed operating information.

Refer to Figure 2 to visualize the interconnection of the equipment in the ground station. Figure 27 shows a photograph of the ground station control point.

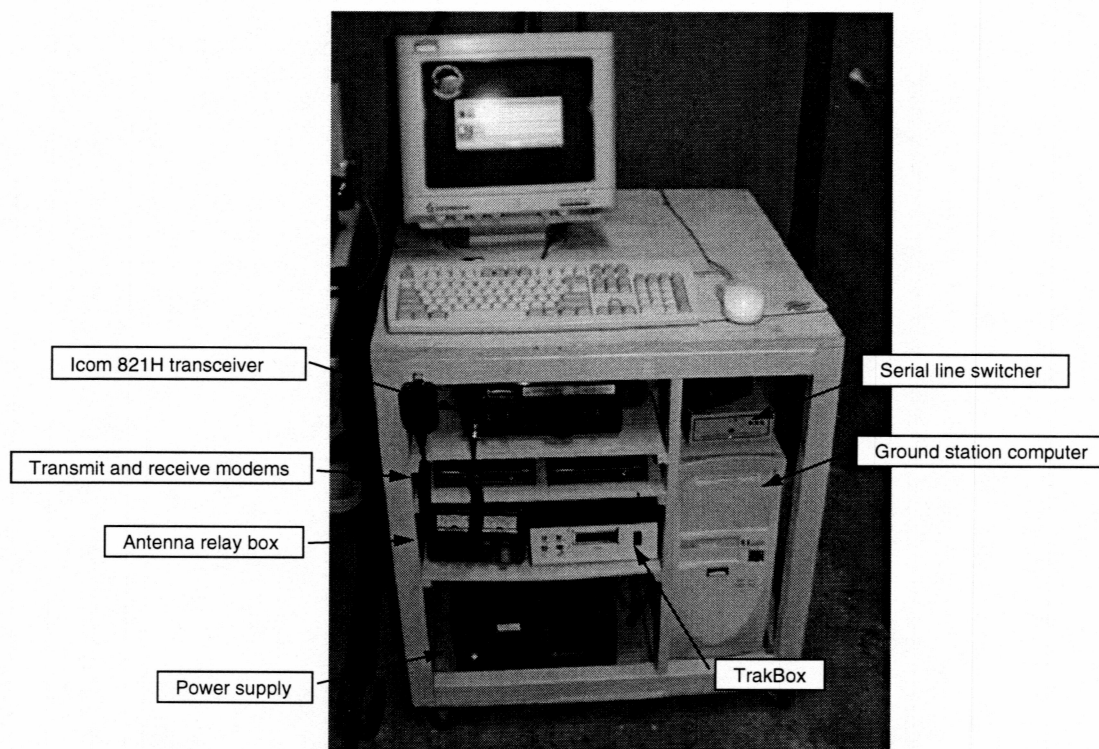


Figure 27: Photograph of ground station equipment

### Computer

The computer that served as the heart of the ground station was a 233 MHz IBM-compatible personal computer. Its operating system was a Redhat 6.1 distribution of Gnu-Linux with kernel version 2.2.13. The important hardware installed in the computer was a Ethernet network interface card and three serial ports. There are three peripheral pieces of equipment that the computer needs to communicate with via serial lines, therefore an extra serial port card was installed in the computer in addition to the two that are part of the computer's motherboard. The computer's BIOS setting

had to be modified to reflect the addition of the ISA serial card. The addition of the serial card caused an IRQ conflict with the motherboard's serial ports, so the serial card was modified to use IRQ 5.

Relevant software packages used in the ground station computer are as follows:

**Point to Point Protocol (PPP)** PPP is available with the Linux distribution used. Configuration files needed to be created for PPP to work properly.

**Minicom** This is a serial port communication program used to configure the packet controller/modems and is available with Linux distributions.

**SatTrack v3.1** This was obtained from [www.amsat.org](http://www.amsat.org), but needed to be modified for Y2K compliance. Some source code files, configuration files, and an orbital element download script needed to be modified for SatTrack to work properly.

The network interface card is essential for allowing the Citizen Explorer project team in Colorado to interface to CX-1 station via the internet. This is a fairly standard feature on many PC's and details about it are therefore omitted.

### Transceiver

The transceiver chosen was an ICOM 821H amateur transceiver, ideally suited for this application. It is a dual band transceiver, capable of full duplex operations between the amateur 2 meter and 70 centimeter bands. It contains both a receiver and transmitter for each band.

Table IV lists some of the transceiver's specifications. The transceiver requires several special

Table IV: ICOM 821H transceiver specifications

Transmit Frequencies	140 - 160 MHz/440 - 460 MHz
Receive Frequencies	140-160 MHz/440 - 460 MHz
Transmit Power	6 - 45 Watts/6 - 25 Watts
Receive Sensitivity (FM)	0.2 $\mu$ V
Direct modulation input level	1 Vpp
Input Power	13.8 Vdc, 16 A

settings to work properly in the ground station. These include turning on the 9600 bps packet functions and routing the proper band receiver output to the packet connection on the back of the

transceiver. The details are found in the manual. In addition, there is a 'Satellite' mode that the transceiver is required to be in for proper routing of the modulator/discriminator signals.

### **Level Converter**

The satellite tracking software used a serial port to instruct the transceiver which frequencies to use. The serial port RS232 levels are  $\pm 12$  Volts, however the transceiver had a TTL serial port with 0/5 Volt levels. The level converter converted data between these two levels.

### **Packet Controller/Modem**

The packet controller/modems are devices with two separate functions in one package. The specific model used in the ground station is a 'Timewave PK96 9600 baud packet controller'.

The point-to-point protocol program communicates via one of the serial ports on the computer. This serial stream of PPP packets from the computer is converted to Unnumbered Information (UI) AX.25 packets by the packet controller. The AX.25 packets are then symbol shaped to provide FSK modulation when applied to the transceiver's modulation input. Reciprocally, AX.25 packets received by the modem are decoded to PPP packets and passed to the computer. The packet controller/modem can be summarized as an interface between the computer and the transceiver.

This was not a typical application of the AX.25 protocol. AX.25 was designed to be a link-control protocol, capable of establishing packet connections to certain points, routing packets in a defined manner, and providing data transfer integrity. In this application, none of the low level AX.25 link control capabilities are used. Instead, PPP was used to establish the connection.

To cause the packet controller/modems to operate in the desired manner, they were placed in a transparent mode, using 'Minicom' to communicate with the devices. Normally, a user interfaces with the command mode of a packet controller. Other typical packet controller modes are 'Host' and 'KISS' (Keep It Simple, Stupid) modes, however these were not employed because the Linux kernel's method of using this serial port is via PPP instead of some other software.

The first choice of packet controller/modem was Paccomm Spirit-2, but when used in transparent mode, this model exhibited severe reliability problems - severe enough that it could not be used in this project.

### **TrakBox**

The 'TrakBox' was an interface between the computer and the antenna motor relay box, which came as a kit. The TrakBox can be an independent satellite tracking device if current orbital elements are entered into it using a serial terminal program. However, the tracking was done by the SatTrack software, so the function of the TrakBox was to interface between SatTrack and the antenna motor relay box.

The TrakBox had two serial port modes, a command mode and a host mode. In command mode, one could directly control the antennas, perform steering calibrations, etc. In host mode, the TrakBox listened on the serial line for antenna steering commands. Once properly calibrated, the TrakBox was placed in host mode, where it remained for normal operation.

The connection to the relay box includes motor outputs and analogue antenna position inputs. The TrakBox compares the voltage from the motors' potentiometers to calibrated position values and asserts the motor control lines accordingly.

### **Power Supply**

Most of the equipment in the ground station used 12 Vdc, including the main load - the transceiver. A high capacity (35 A) power supply was used to provide low voltage power, an Astron RS-35A.

### **Lightning Arrestors and Grounding**

The antenna structure itself was grounded to help avoid equipment damage from lightning. To further reduce this risk, lightning arrestors and a low impedance ground were used in the ground station. The lightning arrestors were devices that normally allowed RF and antenna motor signals to pass through them, but would short signal lines to ground in the event of a large voltage on the signal line.

### **Preamplifier**

In accordance with the downlink budget, a preamplifier was placed on the downlink antenna. This was an Advanced Receiver Research (ARR) MSP432VDG with about 16 dB of gain and a noise figure of about 1 dB. It required 12 Vdc power, which was supplied by the transceiver on the coaxial feed cable.

### Coaxial Signal Cabling

The choice of cable type for the cable runs between the ground station and antennas was based on three criteria: loss, flexibility, and cost. The cable length required between ground station and antennas was approximately 30 meters, enough distance to yield significant cables losses, so a low-loss cable was an important selection. Table V shows typical cable attenuation for different 50  $\Omega$  'RG' types of cable.

Table V: Attenuation for different 50  $\Omega$  cable types

50 $\Omega$ Cable type	loss/100'@100 MHz	loss/100'@400 MHz
RG-405/U	6.5 dB	13 dB
RG-402/U	3.0 dB	7.0 dB
RG-8/U	1.7 dB	3.9 dB
RG-58/U	5 dB	12 dB
RG-213/U	2.1 dB	4.8 dB
RG-214/U	1.9 dB	4.1 dB

This shows that RG-8/U can be expected to have the least loss between these cable types. Manufacturers produce cables to meet 'RG' specifications, and Table VI shows some RG-8/U cables produced by Belden.

Table VI: RG-8/U cables produced by Belden

RG-8/U cable	loss/100'@100 MHz	loss/100'@400 MHz
89913	1.6 dB	3.4 dB
9258	3.9 dB	7.6 dB
9913	1.3 dB	2.7 dB
9913F	1.6 dB	3.5 dB
9888	1.8 dB	4.2 dB
9914	1.6 dB	3.5 dB
8214	1.7 dB	3.9 dB

This table shows that 9913 cable has the lowest loss, followed by the version of 9913 designed for flexibility, 9913F. Cabling to the steerable antenna must remain flexible through winters in Fairbanks, therefore 9913F was selected. This cable is readily available, making it a cost effective selection.



## 7 Conclusions

In the process of putting together this ground station, several important lessons were learned. The protocol method chosen to interface to the spacecraft was not ideal. There were tools readily available in Linux to assign a network interface to a radio modem, without the need for link negotiation and establishment, as in the point to point protocol. Valuable time will be lost in PPP link negotiation and establishment before TCP/IP traffic between ground station and spacecraft. An alternative to this would have been to use well established amateur methods for assigning a network interface to a packet controller/modem. This was not done because methods to do this were not available for VxWorks, the spacecraft's operating system. However, the point to point protocol was readily available for VxWorks, and hence the decision to use PPP instead of other methods.

In addition, since other methods have been available for assigning network interfaces to packet controller/modems, the available amateur hardware is not commonly used to support PPP. This manifested itself when packet controllers did not behave reliably when used as transparent bidirectional data devices. Problems such as freezing up and data loss became evident with different models of packet controller/modems. This furthers the argument for developing AX.25 network interface tools for VxWorks.

Although it is expected that TCP will be tunable to operate acceptably for this project, there is another transport - level protocol that may be more appropriate. Though currently in the test phase, the Space Communications Protocol Standard (SCPS) would be much better suited for spacecraft communications than TCP. SCPS does not assume that packet loss is due solely to congestion and markedly outperforms TCP in links with higher error rates [Ernst '96].

## A Measuring Effects of Intersymbol Interference and Non-linear Channel Effects

This section describes how the contribution of intersymbol interference (ISI) and non-linear channel effects contributed to the probability of bit error. This measured the contribution to bit error probability from the equipment used in the communication link. Given sufficient bandwidth, intersymbol interference can be completely avoided, at least in theory. For a given symbol rate (which is equal to the bit rate in binary modulation schemes, as in non-coherently detected GMSK). The minimum amount of bandwidth required to recover the signal without ISI is [Sklar '88]

$$BW = \frac{R_s}{2} \quad (25)$$

where  $R_s$  is the symbol rate and  $BW$  is the baseband absolute<sup>16</sup> bandwidth. However, this is valid for an ideal and unrealizable “brick wall” low pass filter. Even with enough bandwidth, improper symbol shaping or channel filtering can lead to ISI.

In addition, the equipment may not have a linear channel response, which generates intermodulation products and distorts the original signal, adding to the bit error probability. In this test, no effort was made to distinguish the effects of intersymbol interference from nonlinear channel effects. Their net contribution to bit error rate was measured together.

Since BER test equipment was not available, a measurement method had to be developed. Figure A.1 illustrates the setup used for this test. This implies two nested link layers, one between packet controllers/modems and one between transceivers. Note that, ideally, the radio channel appears as a transparent channel between packet controllers/modems.

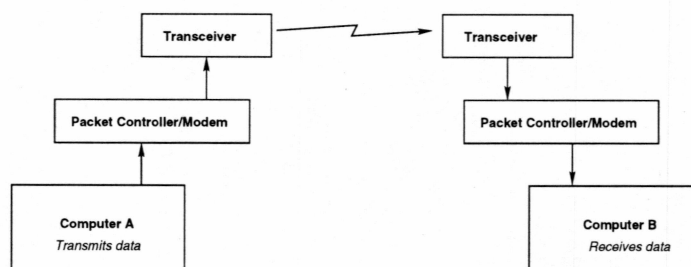


Figure A.1: Setup for measuring bit error rate

<sup>16</sup> Absolute bandwidth refers to any non-zero response

To gather data on bit error rate, a binary file was dumped to the serial port of Computer A while Computer B recorded incoming data to a file from its serial port. In other words, one computer transmitted data with no regard to how well it was received and the other computer simply recorded what came in the serial port.

First, Computer B was instructed to record its serial port data with the Linux command

```
#cat /dev/modem > datafile
```

then Computer A was issued the command

```
#cat datafile > /dev/modem
```

The recorded file sizes were compared to the original file size. With the setup of Figure A.1, it was found that the average recorded file size was about 82% of the original file size.

To relate this datum to bit error probability, one must look at how the AX.25 protocol forms and recovers data packets. Figure A.2 shows the structure of an AX.25 packet. The number of

Flag	Address	Control	Info	FCS	Flag
01111110	112/224 Bits	8/16 Bits	N*8 Bits	16 Bits	01111110

Figure A.2: AX.25 'Unnumbered Information' packet structure.

data bytes inserted into each frame is a configurable parameter within the packet controllers. Upon receiving a packet, an AX.25 packet controller uses the Frame Check Sequence (FCS) to determine whether or not the packet has been corrupted. If it has been corrupted by one or more bits, the packet controller disregards the frame and does not pass the data along to the computer [Beech '97]. In other words, no error correction takes place, only error detection. The probability that errors are not detected is low, over 99.998% of corrupted frames will be detected with the 16-bit FCS. This makes it relatively easy to correlate packet corruption probability with bit error probability by neglecting the possibility that corrupted packets contributed to the recorded file size.

Disregarding the possibility that errors go undetected in a packet, the probability of a packet being received intact is the product of its constituent bits being received intact. This may be expressed as

$$P_r(\text{packet intact}) = P_r(\text{bit intact})^{N_p} \quad (26)$$

where  $P_r(\text{packet intact})$  was the measured probability of receiving a packet correctly,  $P_r(\text{bit intact})$  was the bit-not-in-error probability ( $1 - P_r(\text{bit error})$ ), and  $N_p$  was the number of bits per packet. It follows that the bit error probability can be expressed as

$$P_r(\text{bit error}) = 1 - P_r(\text{packet intact})^{N_p^{-1}} \quad (27)$$

This assumes that the reception of each bit is an independent process: the value of a certain bit has no effect upon the probability of decoding the subsequent bit. This defines intersymbol interference, but this was assumed to be negligible for these calculations.

In order to demonstrate that Equation 27 is valid, Matlab was used to simulate correspondence between Bit Error Rate and packet success rate. Random errors were introduced to a data set at prescribed bit error rates and analysis was done to yield the rate of packet corruption. The results are shown in Figure A.3

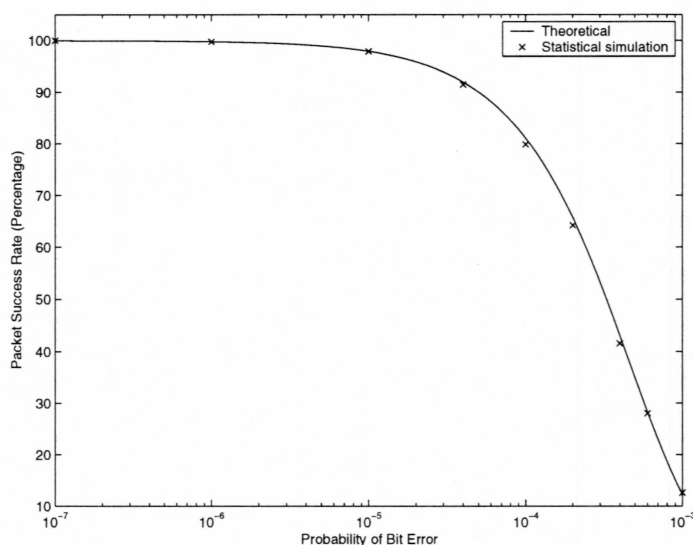


Figure A.3: Simulation results validating the derived relationship between packet success rate and probability of bit error.

Therefore, using the datum of 82% packet success rate and packet size of 2500 bits yields a bit error rate of about  $8 \times 10^{-5}$ .

In addition to this test, the transceivers were removed from the link and the bit error probability from the packet controller/modems communicating over regular wire was measured. The resulting

packet success rate was about 99.9988% which corresponds to a bit error rate of  $6 \times 10^{-9}$ . This is negligible compared to the bit error rate the transceivers introduce.

## B Measuring Receiver Noise Temperature

The effective receiver noise temperature is not commonly available for consumer radio products. This section describes the method used to determine the effective noise figure of the ground station receiver which is illustrated in Figure B.4.

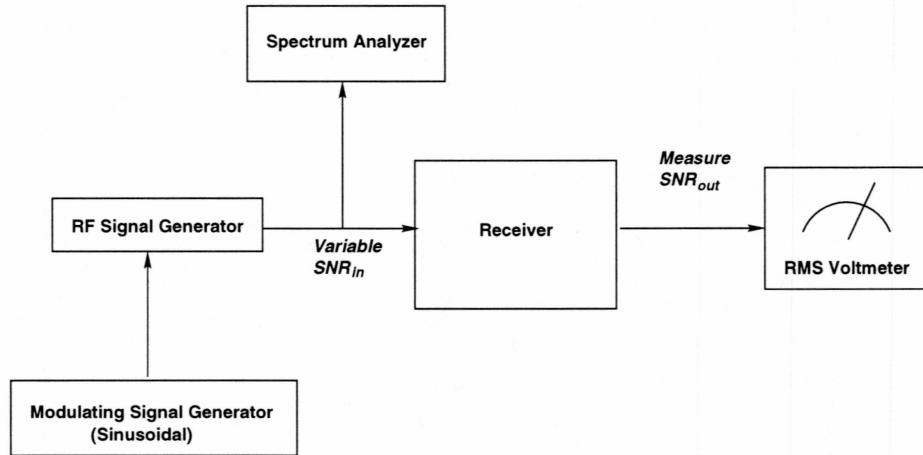


Figure B.4: Set up for measuring receiver noise temperature

The method used involved frequency modulating a carrier with a sinusoidal signal at a known index of modulation  $\beta$  and comparing the empirical signal-to-noise data to the theoretical. A modulation index of 2.4 was used because this value corresponds to the first carrier null, evident from Bessel curves related to FM modulation [Ziemer '95]. A carrier null is easy to discern on a spectrum analyzer. The modulating signal level and frequency were adjusted for the first carrier null ( $\beta = 2.4$ ) and so that most of the spectral energy fit into the receiver bandwidth of 15 kHz.

A noise source was not available, so the inherent black body noise of the Hewlett-Packard 8780A RF signal generator was used. The output terminals of the RF signal generator had a purely resistive impedance of  $50 \Omega$ . If a matched load is connected, the noise power available to a 15 kHz bandwidth is [Sklar '88]

$$N = kTW \cong -132 \text{ dBm} \quad (28)$$

where  $k$  is Boltzmann's constant and  $W$  is the receiver IF half power bandwidth, measured to be 15 kHz. This represents the minimum amount of noise power theoretically available. A real signal source will contribute some amount of added noise, however, this value was not available. If one



disregards any added noise from the source, the results for the receiver noise temperature represent a worst case value.

Knowing the thermal noise power density and the RF signal power out of the signal generator, the signal-to-noise-ratio ( $SNR_{in}$ ) at the terminals of the RF signal generator was

$$SNR_{in} = RF_{out} - 132 \text{ dBm} \quad (29)$$

where  $RF_{out}$  was the RF signal level from the RF generator. In this manner, variable signal to noise ratios were fed to the receiver by varying the RF signal level to the receiver.

The signal-to-noise-ratio out of the receiver was found by observing the rms voltage levels available from the detector. For a given RF signal input level, the modulation was toggled on and off to observe detected noise power and detected signal-plus-noise power. The signal power for each case was found by subtracting the noise power from the signal-plus-noise power. The signal-to-noise-ratio from the receiver detector ( $SNR_{out}$ ) was then the ratio of detected signal power to detected noise power.

For an ideal FM receiver that adds no noise to a signal, the relationship between  $SNR_{out}$  and  $SNR_{in}$  is known [Ziemer '95] and was plotted with the empirical data shown in Figure B.5. For

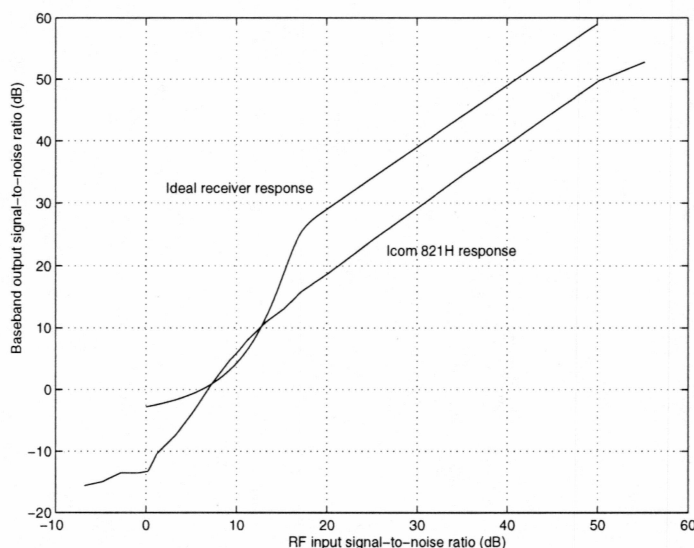


Figure B.5: Ideal and empirical data for determining receiver noise figure

above threshold, to attain a given  $SNR_{out}$  requires about 10 dB more signal for the ground station

receiver than the ideal receiver. This is equivalent to saying that the receiver noise figure is 10 dB. Noise temperature  $T_r$  is related to noise figure by

$$T_r = (F_r - 1)290 \text{ K} \quad (30)$$

and thus  $T_r$  was 2610 K.

## C Downlink Budget Calculations

### Physical Constants

Speed of light in free space	$c = 3.0 \times 10^8 \frac{\text{m}}{\text{s}}$
Boltzmann's constant	$k = 1.38 \times 10^{-23} \frac{\text{J}}{\text{K}}$
Signal frequency	$f = 436.75 \text{ MHz}$
Signal wavelength	$\lambda = \frac{c}{f} = 69 \text{ cm}$
Orbital height	$h = 706 \text{ km}$
Earth Radius	$R_e = 6370 \text{ km}$

### Satellite Transmit

Power	$P_t = 2 \text{ Watts}$
	$P_{dB} = 10 \log(P_t) = 3.0 \text{ dBW}$
Antenna Gain	$G_t = 2 \text{ dB}$
Line loss	$L = 1 \text{ dB}$
Effective Isotropic Radiated Power	$EIRP = P_{dB} + G_t - L = 4.0 \text{ dBW}$

### Propagation

Angle of elevation	$\Phi = 45^\circ \frac{\pi}{180^\circ} \text{ radians}$
	$\Theta = \Phi + \frac{\pi}{2} \text{ radians}$
Slant range	$R = R_e \cos(\Theta) + \sqrt{R_e^2 \cos^2(\Theta) + 2R_e h + h^2} = 952 \text{ km}$
Path loss	$L_p = \left(\frac{4\pi R}{\lambda}\right)^2$
	$L_{dB} = 10 \log(L_p) = 144.8 \text{ dB}$
Propagation loss	$P = L_{dB} = 144.8 \text{ dB}$

**Ground Station Receive**

Antenna Gain	$G_r = 17$ dBi
Pointing loss	$\eta_{pointing} = 0.5$ dB
Polarization loss	$\eta_{pol} = 0$ dB
Total reception gain	$R_x = G_r - \eta_{pointing} - \eta_{pol} = 16.5$ dB
Pre-LNA line loss	$L_{1dB} = 0.2$ dB $L_1 = 10^{\frac{L_{1dB}}{10}}$
Pre-LNA line loss noise temperature	$T_{L_1} = (L_1 - 1)290$ K = 14 K
LNA noise figure	$F_{LNA_{dB}} = 1$ dB $F_{LNA} = 10^{\frac{F_{LNA_{dB}}}{10}}$
LNA noise temperature	$T_{LNA} = (F_{LNA} - 1)290 = 75$ K
LNA Gain	$G_{LNA_{dB}} = 16$ dB $G_{LNA} = 10^{\frac{G_{LNA_{dB}}}{10}}$
Post LNA line loss	$L_{2dB} = 5$ dB $L_2 = 10^{\frac{L_{2dB}}{10}}$
Post LNA line loss noise temperature	$T_{L_2} = (L_2 - 1)290 = 627$ K
Receiver noise temperature	$T_r = 2610$ K
Net receiver noise temperature	$T_R = T_{L_1} + L_1 T_{LNA} + \frac{T_{L_2} L_1}{G_{LNA}} + \frac{T_r L_1 L_2}{G_{LNA}} = 326$ K
Antenna noise temperature	$T_A = 70$ K
System noise temperature	$T_{sys} = T_R + T_A = 396$ K
Received noise power density	$N_o = kT_{sys}$ $N_{o_{dB}} = 10 \log(N_o) = -203$ dBW/Hz
Received signal power	$C = EIRP - P + R_x = -124.3$ dBW
Received power to noise power density ratio	$\frac{C}{N_o} = 77.7$ dBHz

**Digital**

Data rate	$R = 9600 \text{ bps}$ $R_{dB} = 10 \log R = 40 \text{ dBbps}$
Received $\frac{E_b}{N_o}$	$\left(\frac{E_b}{N_o}\right)_{received} = \frac{C}{N_o} - R_{dB} = 37.9 \text{ dB}$
Maximum allowed BER due to noise	$P_r = 1 \times 10^{-7}$
Degradation from MSK	$d_{MSK} = -2 \text{ dB} = 0.63$
$\frac{E_b}{N_o}$ required to achieve $P_r$	$\left(\frac{E_b}{N_o}\right)_{required} = \frac{-2 \ln(2P_r)}{d_{MSK}}$ $\left(\frac{E_b}{N_o}\right)_{required_{dB}} = 10 \log \left(\frac{E_b}{N_o}\right)_{required} = 16.9 \text{ dB}$
Noise BER margin	Margin = $\left(\frac{E_b}{N_o}\right)_{required_{dB}} - \left(\frac{E_b}{N_o}\right)_{received} = \boxed{18 \text{ dB}}$

## References

- [Allman '97] Allman, Mark, *Thesis Entitled Improving TCP Performance Over Satellite Channels*, Ohio University, June 1997
- [Beech '97] Beech, William, Nielsen, Douglas, and Taylor, Jack, *AX.25 Link Access Protocol for Amateur Packet Radio*, Tucson Amateur Packet Radio Corporation, p1-17, 1997
- [Chobotov '91] Chobotov, Vladimir, *ORBITAL MECHANICS*, American Institute of Aeronautics and Astronautics, 1991, p212, 248-249
- [Comer '99] Comer and Stevens, *INTERNETWORKING WITH TCP/IP*, Prentice Hall, p299-300, 1999
- [Ernst '96] Ernst and Durst, *Space Communications Protocol Standard - Bent Pipe Report*, May 1996
- [Ho '70] Ho and Yeh, *A New Approach for Evaluating the Error Probability in the Presence of Intersymbol Interference and Additive Gaussian Noise*, The Bell System Technical Journal, p2251, November 1970
- [Kraus '88] Kraus, John, *ANTENNAS*, McGraw Hill, p265-338, 1988
- [Murota '81] Murota and Hirade, *GMSK Modulation for Digital Mobile Radio Telephony*, IEEE Transactions on Communication, p1045-1049, July 1981
- [Paccomm '94] Paccomm Radio Systems, *Spirit-2 (GMSK modem) Technical Reference Manual*, , p9, 1994
- [Pratt '86] Pratt, Timothy, and Bostian, Charles, *SATELLITE COMMUNICATIONS*, John Wiley & Sons, p186-192, 1986
- [RFC 1661] Request For Comments (RFC) 1661 - *The Point to Point Protocol* , W. Simpson, p1-9, July 1994
- [RFC 1662] Request For Comments (RFC) 1662 - *PPP in HDLC-like Framing*, W. Simpson, p1-7, July 1994



- [Sklar '88] Sklar, Bernard, DIGITAL COMMUNICATIONS, Prentice Hall, p98-102, 152-154, 403-407, 1988
- [Stallings '97] Stallings, William, DATA AND COMPUTER COMMUNICATIONS, Prentice Hall, p20, 176-185, 402, 497-526, 1997
- [Ziener '95] Ziener and Tranter, PRINCIPLES OF COMMUNICATION, John Wiley & Sons, p414-431, 1995